

Hybrid Transceiver Optimization for Multi-Hop Communications

Chengwen Xing, *Member, IEEE*, Xin Zhao, Shuai Wang, Wei Xu, *Senior Member, IEEE*,
Soon Xin Ng, *Senior Member, IEEE*, and Sheng Chen, *Fellow, IEEE*

Abstract—Multi-hop communication with the aid of large-scale antenna arrays will play a vital role in future emergence communication systems. In this paper, we investigate amplify-and-forward based and multiple-input multiple-output assisted multi-hop communication, in which all nodes employ hybrid transceivers. Moreover, channel errors are taken into account in our hybrid transceiver design. Based on the matrix-monotonic optimization framework, the optimal structures of the robust hybrid transceivers are derived. By utilizing these optimal structures, the optimizations of analog transceivers and digital transceivers can be separated without loss of optimality. This fact greatly simplifies the joint optimization of analog transceivers and digital transceivers. Since the optimization of analog transceivers under unit modulus constraints is non-convex and difficult to solve, a projection type algorithm is proposed for analog transceiver optimization to overcome this difficulty. Based on the derived analog transceivers, the optimal digital transceivers can then be derived using matrix-monotonic optimization. Numerical results are given to demonstrate the performance advantages of the proposed hybrid transceiver designs over other existing solutions.

Index Terms—Hybrid transceiver optimizations, matrix-monotonic optimization, multi-hop communication, emergence communications, linear transceiver, nonlinear transceiver

I. INTRODUCTIONS

Emergency communications are of critical importance in managing emergency scenarios, such as natural disasters, anti-terrorist wars, large-scale sport events, and so on [1]. Multi-hop communication is an important enabling technology for emergency communications because it is less demanding on network infrastructures. For example, multi-hop communications can occur between multiple satellites or multiple unmanned aerial vehicles or other high latitude platforms [2], [3]. Moreover, multi-hop communication is also a promising technology to overcome deep fading over long distance for high frequency band communications, such as millimeter wave communications or Terahertz communications [4]–[8].

Generally speaking, it is challenging to simultaneously guarantee the high reliability and high spectrum efficiency of multi-hop communications [9]. Because of its high spatial diversity and multiplexing gains, the large-scale antenna array technology offers a promising candidate for this difficult task.

It is worth highlighting that different from cellular communications, the physical-size constraints on emergence communication nodes are less stringent. As a result, it is promising to take advantage of multiple-input multiple-output (MIMO) technology to overcome path loss and to improve spectral efficiency simultaneously. For MIMO multi-hop communications, various signal processing strategies at relays can be classified into two categories, i.e., regenerative operation and nonregenerative operation. For a regenerative scheme, at each relay the signal received from the preceding hop is decoded first and a new transmission for the decoded information is performed for the next hop. For a nonregenerative scheme, the received signal from the preceding hop is not decoded but is directly forwarded to the next hop after multiplying it with a forward matrix. Nonregenerative schemes are characterized by their low complexity and high security [6].

In order to satisfy data hungry applications, the scale of MIMO has become larger and larger [10], and correspondingly the cost of antenna arrays in MIMO communication systems has increased dramatically. In particular, the deployment of large-scale antenna arrays will inevitably increase the cost and complexity of emergence communication nodes [11]. In order to reduce the complexity while maintaining performance gains, hybrid structures have attracted lots of attention [12]. Unlike traditional full digital systems, where each antenna is associated with a dedicated radio frequency (RF) chain, in hybrid structures, the number of antennas is much larger than the number of RF chains [13]. For hybrid transceiver designs, the main challenge comes from the analog transceiver optimizations. This is because the unit-modulus constraints on each element of analog transceiver matrices are nonconvex and difficult to deal with [14].

There exist a rich body of literature [13]–[16], which deal with hybrid transceiver designs and investigate performance potentials of hybrid transceivers. In particular, hybrid transceivers are designed for various communication systems, including point-to-point MIMO systems, multi-user MIMO systems [17], dual-hop amplify-and-forward (AF) MIMO systems [18]–[20]. The works [21], [22] show that hybrid structures are capable of striking elegant tradeoffs between complexity and performance. Based on hybrid structures, performance boost coming from large-scale antenna arrays becomes realizable under practical hardware and physical constraints [23]–[25].

Different from these existing works, in this work we investigate the hybrid transceiver designs for multi-hop AF MIMO cooperative networks [26], [27]. Furthermore, channel errors are also taken into account [28]. More specifically, we propose a comprehensive unified framework of robust

C. Xing, X. Zhao and S. Wang are with School of Information and Electronics, Beijing Institute of Technology, Beijing 100081, China (E-mails: chengwenxing@ieee.org, xinzhao.eecs@gmail.com, swang@bit.edu.cn).

W. Xu is with the National Mobile Communications Research Laboratory, Southeast University, Nanjing, China (E-mail: wxu@seu.edu.cn).

S. X. Ng and S. Chen are with School of Electronics and Computer Science, University of Southampton, U.K. (E-mails: sxn@ecs.soton.ac.uk, sqc@ecs.soton.ac.uk). S. Chen is also with King Abdulaziz University, Jeddah, Saudi Arabia.

hybrid transceiver optimizations for multi-hop cooperative communications. Our work is much more challenging than the existing works. The main contributions of this work are listed as follows, which differentiate our work from the existing works distinctly.

- We consider a general multi-hop AF MIMO relaying system, where multiple relays facilitate the communications between source and its destination. All nodes are equipped with multiple antennas and multiple data streams are simultaneously transmitted. In addition, both linear transceivers and nonlinear transceivers are investigated in our framework. The nonlinear transceivers investigated include Tomlinson-Harashima precoding (THP) at the source or decision feedback equalizer (DFE) at the destination [29]–[31].
- For the linear transceiver designs of multi-hop AF MIMO relaying networks, two general types of performance metrics are considered, namely, additively Schur-convex function and additively Schur-concave function of the diagonal elements of the data estimation matrix at the destination. Different fairness levels can be realized by using these two types of performance metrics.
- For the nonlinear transceiver designs of multi-hop AF MIMO relaying networks, two general kinds of performance metrics are considered, namely, multiplicatively Schur-convex function and multiplicatively Schur-concave function of the diagonal elements of the data estimation matrix at the destination. Different fairness levels can be realized by using these two kinds of performance metrics.
- In our work, the channel errors in each hop are taken into account. Moreover, the correlated channel errors are considered. The correlated channel errors make the hybrid transceiver optimization for AF MIMO relaying networks particularly challenging, and to the best of our knowledge, this robust hybrid transceiver optimization has not been addressed in existing literature.
- At source and destination, the hybrid transceiver consists of two parts, i.e., analog precoder and digital precoder as well as analog receiver and digital receiver, respectively. At each relay, the hybrid transceiver consists of three components, i.e., analog receive part, digital forward part and analog transmit part. Based on the matrix-monotonic framework [26], the optimal structures of these three components are derived. By exploiting these optimal structures, the robust hybrid transceiver for multi-hop communications is optimized efficiently. Our results can be applied to any frequency bands, including microwave, millimeter wave and Terahertz frequency bands.

Throughout our discussions, bold-faced lower-case and upper-case letters denote vectors and matrices, respectively. The Hermitian square root of a positive semi-definite matrix \mathbf{M} is denoted by $\mathbf{M}^{\frac{1}{2}}$. The expectation operator is denoted by $\mathbb{E}\{\cdot\}$ and $\text{Tr}(\cdot)$ is the matrix trace operator, while $(\cdot)^T$, $(\cdot)^*$, $(\cdot)^H$ and $(\cdot)^{-1}$ denote transpose, conjugate, Hermitian transpose and inverse operators, respectively. The diagonal matrix with the diagonal elements $\lambda_1, \dots, \lambda_N$ is denoted

as $\text{diag}\{\lambda_1, \dots, \lambda_N\} = \text{diag}\{[\lambda_1 \dots \lambda_N]^T\}$, and \mathbf{I} denotes the identity matrix of appropriate dimension, while $\mathbf{d}[\mathbf{M}]$ is the vector whose elements are the diagonal elements of matrix \mathbf{M} , and $\mathbf{d}^2[\mathbf{M}] = \mathbf{d}[\text{diag}\{\mathbf{d}[\mathbf{M}]\}\text{diag}^*\{\mathbf{d}[\mathbf{M}]\}]$. The real part of scalar/matrix is denoted by $\Re\{\cdot\}$, and the angle of scalar a is denoted as $\angle a$. The symbol $\mathcal{P}_{\mathcal{F}}\{\cdot\}$ denotes the angle projection operation, i.e., $\mathcal{P}_{\mathcal{F}}\{a\} = e^{j\angle a}$, where $j = \sqrt{-1}$, and $\|\cdot\|_F$ is the matrix Frobenius norm. The symbol $\mathbf{\Lambda} \searrow$ represents a rectangular or square diagonal matrix whose diagonal elements are arranged in decreasing order, while $\boldsymbol{\lambda}\{\mathbf{M}\} = [\lambda_1(\mathbf{M}) \ \lambda_2(\mathbf{M}) \ \dots \ \lambda_N(\mathbf{M})]^T$, where $\lambda_n(\mathbf{M})$ is the n th largest eigenvalue of the $N \times N$ matrix \mathbf{M} . Furthermore, $(a)^{\dagger} = \max\{0, a\}$. The words ‘independently and identically distributed’ and ‘with respect to’ are abbreviated as ‘i.i.d.’ and ‘w.r.t.’, respectively.

II. SYSTEM MODEL AND PROBLEM FORMULATION

We consider a general multi-hop (K -hop) AF MIMO relaying network in which multiple ($K - 1$) relay nodes (denoted by nodes 1 to $K - 1$) help a source node (denoted as node 0) to communicate with a destination node (denoted as node K). At each relay, the received signal vector is not decoded but is directly forwarded to the next node after multiplying it with a forward matrix. All the nodes are equipped with multiple antennas and multiple data streams are simultaneously transmitted.

Let the transmitted signal vector from the source be \mathbf{x}_0 with $\mathbb{E}\{\mathbf{x}_0 \mathbf{x}_0^H\} = \sigma_0^2 \mathbf{I}$. Then in the k th hop, where $1 \leq k \leq K$, the received signal vector at the k th node can be expressed as

$$\mathbf{x}_k = \mathbf{H}_k \mathbf{F}_k \mathbf{x}_{k-1} + \mathbf{n}_k, \quad (1)$$

where \mathbf{H}_k is the k th hop channel matrix, \mathbf{x}_{k-1} is the transmitted signal vector from the preceding node, and \mathbf{n}_k is the additive white Gaussian noise (AWGN) vector at the k th node, which has the covariance matrix of $\sigma_{\mathbf{n}_k}^2 \mathbf{I}$, while the forward matrix \mathbf{F}_k for the k th hop satisfies the following hybrid structure

$$\mathbf{F}_k = \mathbf{F}_{\text{AL},k} \mathbf{F}_{\text{D},k} \mathbf{F}_{\text{AR},k}, \quad (2)$$

in which $\mathbf{F}_{\text{AL},k}$, $\mathbf{F}_{\text{D},k}$ and $\mathbf{F}_{\text{AR},k}$ are the analog transmit precoder matrix, digital forward matrix, and analog receive combiner matrix for the k th hop or the $(k - 1)$ th node, respectively. In particular, $\mathbf{F}_{\text{AR},1} = \mathbf{I}$.

In practice, owing to the time varying nature and/or limited training resource, the channel state information (CSI) available at a node is imperfect. Therefore, we model the channel matrix \mathbf{H}_k by

$$\mathbf{H}_k = \widehat{\mathbf{H}}_k + \mathbf{H}_{\text{W},k} \boldsymbol{\Psi}_k^{\frac{1}{2}}, \quad (3)$$

where $\widehat{\mathbf{H}}_k$ is the estimated channel matrix available, and the elements of $\mathbf{H}_{\text{W},k}$ are i.i.d. random variables with zero mean and unit power. The positive semidefinite matrix $\boldsymbol{\Psi}_k$ is the transmit correlation matrix of the channel errors. From the viewpoint of channel estimation, $\boldsymbol{\Psi}_k$ is a function of training sequences. The detailed derivation of $\boldsymbol{\Psi}_k$ is beyond the scope of this paper and the interested readers are referred to [4].

At the destination, i.e., node K , the desired signal \mathbf{x}_0 may be recovered from the noise corrupted observation \mathbf{x}_K via a hybrid linear equalizer, which can be expressed as

$$\hat{\mathbf{x}}_0 = \mathbf{G}_D \mathbf{G}_A \mathbf{x}_K, \quad (4)$$

where \mathbf{G}_D and \mathbf{G}_A denote the digital and analog equalizers of the hybrid equalizer at the destination, respectively. Given the hybrid linear equalizer and all the forward matrices $\{\mathbf{F}_k\}_{k=1}^K$, the corresponding mean squared error (MSE) matrix is defined by [32]

$$\begin{aligned} \Phi_{\text{MSE}}^L(\mathbf{G}_D, \mathbf{G}_A, \{\mathbf{F}_k\}_{k=1}^K) \\ = \mathbb{E}\{(\mathbf{G}_D \mathbf{G}_A \mathbf{x}_K - \mathbf{x}_0)(\mathbf{G}_D \mathbf{G}_A \mathbf{x}_K - \mathbf{x}_0)^H\}. \end{aligned} \quad (5)$$

As there is no constraint for digital equalizer, the optimal digital equalizer \mathbf{G}_D can be derived in closed form [4]. Substituting this optimal \mathbf{G}_D into (5), the corresponding data estimation MSE matrix can be expressed as

$$\begin{aligned} \Phi_{\text{MSE}}^L(\mathbf{G}_A, \{\mathbf{F}_k\}_{k=1}^K) &= \sigma_0^2 \mathbf{I} \\ &- \sigma_0^4 (\mathbf{G}_A \widehat{\mathbf{H}}_K \mathbf{F}_K \widehat{\mathbf{H}}_{K-1}^H \mathbf{F}_{K-1} \cdots \widehat{\mathbf{H}}_1^H \mathbf{F}_1)^H \\ &\times (\mathbf{G}_A \widehat{\mathbf{H}}_K \mathbf{F}_K \mathbf{R}_{\mathbf{x}_{K-1}} \mathbf{F}_K^H \widehat{\mathbf{H}}_K^H \mathbf{G}_A^H + \mathbf{K}_{\mathbf{n}_K})^{-1} \\ &\times (\mathbf{G}_A \widehat{\mathbf{H}}_K \mathbf{F}_K \widehat{\mathbf{H}}_{K-1}^H \mathbf{F}_{K-1} \cdots \widehat{\mathbf{H}}_1^H \mathbf{F}_1), \end{aligned} \quad (6)$$

where $\mathbf{K}_{\mathbf{n}_K}$ is the equivalent noise covariance matrix at the destination, which can be expressed as

$$\mathbf{K}_{\mathbf{n}_K} = \mathbf{G}_A \mathbf{R}_{\mathbf{n}_K} \mathbf{G}_A^H + \text{Tr}(\mathbf{F}_K \mathbf{R}_{\mathbf{x}_{K-1}} \mathbf{F}_K^H \Psi_K) \mathbf{G}_A \mathbf{G}_A^H, \quad (7)$$

while the covariance matrix $\mathbf{R}_{\mathbf{x}_k}$ of \mathbf{x}_k , for $1 \leq k \leq K-1$, is given by

$$\mathbf{R}_{\mathbf{x}_k} = \widehat{\mathbf{H}}_k \mathbf{F}_k \mathbf{R}_{\mathbf{x}_{k-1}} \mathbf{F}_k^H \widehat{\mathbf{H}}_k^H + \mathbf{K}_{\mathbf{n}_k}, \quad (8)$$

in which

$$\mathbf{K}_{\mathbf{n}_k} = \sigma_{\mathbf{n}_k}^2 \mathbf{I} + \text{Tr}(\mathbf{F}_k \mathbf{R}_{\mathbf{x}_{k-1}} \mathbf{F}_k^H \Psi_k) \mathbf{I}. \quad (9)$$

Note that $\mathbf{R}_{\mathbf{x}_0} = \sigma_0^2 \mathbf{I}$.

Based on the analog linear equalized data estimation, nonlinear transceivers can further be implemented for example by using the THP at the source or adopting the DFE at the destination. Let the lower triangular matrix \mathbf{B} be the feedback matrix adopted in the THP or DFE. Then the corresponding data estimation MSE matrix can be expressed as

$$\begin{aligned} \Phi_{\text{MSE}}^{\text{NL}}(\mathbf{B}, \mathbf{G}_A, \{\mathbf{F}_k\}_{k=1}^K) &= (\mathbf{I} + \mathbf{B}) \Phi_{\text{MSE}}^L(\mathbf{G}_A, \{\mathbf{F}_k\}_{k=1}^K) \\ &\times (\mathbf{I} + \mathbf{B})^H. \end{aligned} \quad (10)$$

Based on the data estimation MSE matrices (6) and (10) for linear transceivers and nonlinear transceivers, respectively, the following transceiver optimization problems can be formulated. Specifically, the linear hybrid transceiver optimization for multi-hop communications can be formulated as

$$\begin{aligned} \min_{\mathbf{G}_A, \{\mathbf{F}_k\}_{k=1}^K} & f_L(d[\Phi_{\text{MSE}}^L(\mathbf{G}_A, \{\mathbf{F}_k\}_{k=1}^K)]), \\ \text{s.t.} & \text{Tr}(\mathbf{F}_k \mathbf{R}_{\mathbf{x}_{k-1}} \mathbf{F}_k^H) \leq P_k, \\ & \mathbf{F}_{\text{AL},k} \in \mathcal{F}_{\text{PL},k}, \mathbf{F}_{\text{AR},k} \in \mathcal{F}_{\text{PR},k}, \mathbf{G}_A \in \mathcal{F}_G, \end{aligned} \quad (11)$$

where P_k is the maximum transmit power at the k th node, while $\mathcal{F}_{\text{PL},k}$, $\mathcal{F}_{\text{PR},k}$ and \mathcal{F}_G denote the corresponding analog matrix sets with proper dimensions and the elements of any

matrix in these sets have constant amplitude. The objective function $f_L(\cdot)$ can be an additively Schur-convex or additively Schur-concave function of the diagonal elements of the data estimation MSE matrix $\Phi_{\text{MSE}}^L(\mathbf{G}_A, \{\mathbf{F}_k\}_{k=1}^K)$. Similarly, the nonlinear hybrid transceiver optimization for multi-hop communications can be expressed as

$$\begin{aligned} \min_{\mathbf{G}_A, \{\mathbf{F}_k\}_{k=1}^K} & f_{\text{NL}}(d[(\mathbf{I} + \mathbf{B}) \Phi_{\text{MSE}}^L(\mathbf{G}_A, \{\mathbf{F}_k\}_{k=1}^K) (\mathbf{I} + \mathbf{B})^H]), \\ \text{s.t.} & \text{Tr}(\mathbf{F}_k \mathbf{R}_{\mathbf{x}_{k-1}} \mathbf{F}_k^H) \leq P_k, \\ & \mathbf{F}_{\text{AL},k} \in \mathcal{F}_{\text{PL},k}, \mathbf{F}_{\text{AR},k} \in \mathcal{F}_{\text{PR},k}, \mathbf{G}_A \in \mathcal{F}_G, \end{aligned} \quad (12)$$

where the objective function $f_{\text{NL}}(\cdot)$ is a multiplicatively Schur-convex or multiplicatively Schur-concave function of the diagonal elements of the data estimation MSE matrix $\Phi_{\text{MSE}}^{\text{NL}}(\mathbf{B}, \mathbf{G}_A, \{\mathbf{F}_k\}_{k=1}^K)$.

III. PROBLEM REFORMULATION

In order to simplify the derivations for linear and nonlinear transceiver designs, we first introduce the following auxiliary variables

$$\bar{\mathbf{F}}_1 = \mathbf{F}_1 \mathbf{Q}_0^H, \quad (13)$$

$$\bar{\mathbf{F}}_k = \mathbf{F}_k \mathbf{K}_{\mathbf{n}_{k-1}}^{-\frac{1}{2}} \Sigma_{k-1}^{-\frac{1}{2}} \mathbf{Q}_{k-1}^H, \quad 2 \leq k \leq K, \quad (14)$$

where \mathbf{Q}_k for $0 \leq k \leq K-1$ are unitary matrices with proper dimensions, and for $2 \leq k \leq K$,

$$\Sigma_{k-1} = \mathbf{K}_{\mathbf{n}_{k-1}}^{-\frac{1}{2}} \widehat{\mathbf{H}}_{k-1}^H \mathbf{F}_{k-1} \mathbf{R}_{\mathbf{x}_{k-2}} \mathbf{F}_{k-1}^H \widehat{\mathbf{H}}_{k-1} \mathbf{K}_{\mathbf{n}_{k-1}}^{-\frac{1}{2}} + \mathbf{I}. \quad (15)$$

Therefore, the linear data estimation MSE matrix can be reformulated as

$$\Phi_{\text{MSE}}^L(\mathbf{G}_A, \{\bar{\mathbf{F}}_k\}_{k=1}^K, \{\mathbf{Q}_k\}_{k=0}^{K-1}) = \sigma_0^2 \mathbf{I} - \sigma_0^4 \Upsilon^H \Upsilon, \quad (16)$$

where

$$\begin{aligned} \Upsilon &= \left(\Sigma_{K-1}^{-\frac{1}{2}} \mathbf{K}_{\mathbf{n}_K}^{-\frac{1}{2}} \mathbf{G}_A \widehat{\mathbf{H}}_K \bar{\mathbf{F}}_K \mathbf{Q}_{K-1} \Sigma_{K-1}^{-\frac{1}{2}} \mathbf{K}_{\mathbf{n}_{K-1}}^{-\frac{1}{2}} \widehat{\mathbf{H}}_{K-1}^H \bar{\mathbf{F}}_{K-1} \right. \\ &\quad \left. \cdots \mathbf{Q}_1 \Sigma_1^{-\frac{1}{2}} \mathbf{K}_{\mathbf{n}_1}^{-\frac{1}{2}} \widehat{\mathbf{H}}_1^H \bar{\mathbf{F}}_1 \mathbf{Q}_0 \right), \end{aligned} \quad (17)$$

in which

$$\Sigma_K = \mathbf{K}_{\mathbf{n}_K}^{-\frac{1}{2}} \mathbf{G}_A \widehat{\mathbf{H}}_K \bar{\mathbf{F}}_K \mathbf{R}_{\mathbf{n}_{K-1}} \bar{\mathbf{F}}_K^H \widehat{\mathbf{H}}_K^H \mathbf{G}_A^H \mathbf{K}_{\mathbf{n}_K}^{-\frac{1}{2}} + \mathbf{I}. \quad (18)$$

Based on the reformulated data estimation matrix $\Phi_{\text{MSE}}^L(\mathbf{G}_A, \{\bar{\mathbf{F}}_k\}_{k=1}^K, \{\mathbf{Q}_k\}_{k=0}^{K-1})$, the linear transceiver optimization problem (11) can be re-expressed as

$$\begin{aligned} \min_{\mathbf{G}_A, \{\bar{\mathbf{F}}_k\}, \{\mathbf{Q}_k\}} & f_L(d[\Phi_{\text{MSE}}^L(\mathbf{G}_A, \{\bar{\mathbf{F}}_k\}, \{\mathbf{Q}_k\})]), \\ \text{s.t.} & \text{Tr}(\bar{\mathbf{F}}_k \bar{\mathbf{F}}_k^H) \leq P_k, \\ & \mathbf{F}_{\text{AL},k} \in \mathcal{F}_{\text{PL},k}, \mathbf{F}_{\text{AR},k} \in \mathcal{F}_{\text{PR},k}, \mathbf{G}_A \in \mathcal{F}_G, \end{aligned} \quad (19)$$

where for notational simplification, we have dropped the ranges of $\{\bar{\mathbf{F}}_k\}$ and $\{\mathbf{Q}_k\}$.

Similarly, the nonlinear transceiver optimization problem (12) can be rewritten in the following form

$$\begin{aligned} \min_{\mathbf{G}_A, \{\bar{\mathbf{F}}_k\}, \{\mathbf{Q}_k\}} & f_{\text{NL}}(d[(\mathbf{I} + \mathbf{B}) \Phi_{\text{MSE}}^L(\mathbf{G}_A, \{\bar{\mathbf{F}}_k\}, \{\mathbf{Q}_k\}) \\ & \quad \times (\mathbf{I} + \mathbf{B})^H]), \\ \text{s.t.} & \text{Tr}(\bar{\mathbf{F}}_k \bar{\mathbf{F}}_k^H) \leq P_k, \\ & \mathbf{F}_{\text{AL},k} \in \mathcal{F}_{\text{PL},k}, \mathbf{F}_{\text{AR},k} \in \mathcal{F}_{\text{PR},k}, \mathbf{G}_A \in \mathcal{F}_G. \end{aligned} \quad (20)$$

The optimal lower triangular matrix \mathbf{B} satisfies [6], [30]

$$\mathbf{I} + \mathbf{B}_{\text{opt}} = \text{diag}\{d[\mathbf{L}]\}\mathbf{L}^{-1}, \quad (21)$$

where \mathbf{L} is the lower triangular matrix of the following Cholesky decomposition

$$\Phi_{\text{MSE}}^{\text{L}}(\mathbf{G}_A, \{\bar{\mathbf{F}}_k\}, \{\mathbf{Q}_k\}) = \mathbf{L}\mathbf{L}^H. \quad (22)$$

As a result, the general nonlinear transceiver optimization problem (20) can be rewritten as

$$\begin{aligned} \min_{\mathbf{G}_A, \{\bar{\mathbf{F}}_k\}, \{\mathbf{Q}_k\}} \quad & f_{\text{NL}}(d^2[\mathbf{L}]), \\ \text{s.t.} \quad & \Phi_{\text{MSE}}^{\text{L}}(\mathbf{G}_A, \{\bar{\mathbf{F}}_k\}, \{\mathbf{Q}_k\}) = \mathbf{L}\mathbf{L}^H, \\ & \text{Tr}(\bar{\mathbf{F}}_k \bar{\mathbf{F}}_k^H) \leq P_k, \\ & \mathbf{F}_{\text{AL},k} \in \mathcal{F}_{\text{PL},k}, \mathbf{F}_{\text{AR},k} \in \mathcal{F}_{\text{PR},k}, \mathbf{G}_A \in \mathcal{F}_G. \end{aligned} \quad (23)$$

In the following sections, it is shown that the optimal $\{\mathbf{Q}_k\}$, $\{\bar{\mathbf{F}}_k\}$ and \mathbf{G}_A can be derived separately for both linear transceiver and nonlinear transceiver designs of the multi-hop AF MIMO relay system with different objective functions.

IV. OPTIMAL UNITARY MATRICES

In the new design formulations, the unitary matrices $\{\mathbf{Q}_k\}$ do not appear in the constraints. Based on our previous works [5], [6], we can easily derive the optimal \mathbf{Q}_k for $1 \leq k \leq K-1$, as summarized in the following conclusion.

Conclusion 1 Define the following singular value decompositions (SVDs)

$$\Sigma_k^{-\frac{1}{2}} \mathbf{K}_{\mathbf{n}_k}^{-\frac{1}{2}} \widehat{\mathbf{H}}_k \bar{\mathbf{F}}_k = \mathbf{U}_k \mathbf{\Lambda}_k \mathbf{V}_k^H, \quad 1 \leq k < K, \quad (24)$$

$$\Sigma_K^{-\frac{1}{2}} \mathbf{K}_{\mathbf{n}_K}^{-\frac{1}{2}} \mathbf{G}_A \widehat{\mathbf{H}}_K \bar{\mathbf{F}}_K = \mathbf{U}_K \mathbf{\Lambda}_K \mathbf{V}_K^H. \quad (25)$$

Then the optimal \mathbf{Q}_k for $1 \leq k \leq K-1$ are given by

$$\mathbf{Q}_{k,\text{opt}} = \mathbf{V}_{k+1} \mathbf{U}_k^H. \quad (26)$$

The optimal solution for \mathbf{Q}_0 is a bit complicated as it is determined by the objective function, and we discuss it case by case.

A. Linear Transceiver Designs

Consider the additively Schur-convex objective function for $f_{\text{L}}(\cdot)$, namely,

$$\text{Obj.1} : f_{\text{A-Schur}}^{\text{Convex}}(d[\Phi_{\text{MSE}}^{\text{L}}(\mathbf{G}_A, \{\bar{\mathbf{F}}_k\}, \{\mathbf{Q}_k\})]). \quad (27)$$

Then according to [26],

$$\mathbf{Q}_{0,\text{opt}} = \mathbf{V}_1 \bar{\mathbf{U}}_{\text{DFT}}^H, \quad (28)$$

where the unitary matrix $\bar{\mathbf{U}}_{\text{DFT}}$ is the discrete Fourier transform (DFT) matrix of appropriate dimension, which makes sure that all the diagonal elements of the data estimation MSE matrix are identical. On the other hand, when the objective function is additively Schur-concave, that is,

$$\text{Obj.2} : f_{\text{A-Schur}}^{\text{Concave}}(d[\Phi_{\text{MSE}}^{\text{L}}(\mathbf{G}_A, \{\bar{\mathbf{F}}_k\}, \{\mathbf{Q}_k\})]), \quad (29)$$

we have [26]

$$\mathbf{Q}_{0,\text{opt}} = \mathbf{V}_1. \quad (30)$$

It can be seen that with the additively Schur-concave objective function, the matrix version of the signal-to-noise ratio (SNR) is a diagonal matrix at the optimal solution of $\mathbf{Q}_{0,\text{opt}}$.

Based on the optimal unitary matrices $\{\mathbf{Q}_{k,\text{opt}}\}_{k=0}^{K-1}$, the linear transceiver optimization problem (19) becomes

$$\begin{aligned} \min_{\mathbf{G}_A, \{\bar{\mathbf{F}}_k\}} \quad & f_{\text{L}}\left(\left\{\lambda\left\{\bar{\mathbf{F}}_k^H \widehat{\mathbf{H}}_k^H \mathbf{K}_{\mathbf{n}_k}^{-1} \widehat{\mathbf{H}}_k \bar{\mathbf{F}}_k\right\}\right\}\right), \\ \text{s.t.} \quad & \text{Tr}(\bar{\mathbf{F}}_k \bar{\mathbf{F}}_k^H) \leq P_k, \\ & \mathbf{F}_{\text{AL},k} \in \mathcal{F}_{\text{PL},k}, \mathbf{F}_{\text{AR},k} \in \mathcal{F}_{\text{PR},k}, \mathbf{G}_A \in \mathcal{F}_G, \end{aligned} \quad (31)$$

where again for notational simplification, we have dropped the range of $\left\{\lambda\left\{\bar{\mathbf{F}}_k^H \widehat{\mathbf{H}}_k^H \mathbf{K}_{\mathbf{n}_k}^{-1} \widehat{\mathbf{H}}_k \bar{\mathbf{F}}_k\right\}\right\}$.

B. Nonlinear Transceiver Designs

For the nonlinear transceiver designs with THP or DFE, when the objective function $f_{\text{NL}}(\cdot)$ is multiplicatively Schur-convex w.r.t. the diagonal elements of the data estimation MSE matrix, namely,

$$\begin{aligned} \text{Obj.3} : \quad & f_{\text{M-Schur}}^{\text{Convex}}(d^2[\mathbf{L}]), \\ \text{with} \quad & \Phi_{\text{MSE}}^{\text{L}}(\mathbf{G}_A, \{\bar{\mathbf{F}}_k\}, \{\mathbf{Q}_k\}) = \mathbf{L}\mathbf{L}^H, \end{aligned} \quad (32)$$

the optimal solution of \mathbf{Q}_0 is given by [26]

$$\mathbf{Q}_{0,\text{opt}} = \mathbf{V}_1 \bar{\mathbf{U}}_{\text{GMD}}^H, \quad (33)$$

where the unitary matrix $\bar{\mathbf{U}}_{\text{GMD}}$ makes sure that the lower triangular matrix \mathbf{L} has the same diagonal elements. On the other hand, when the objective function is multiplicatively Schur-concave w.r.t. the diagonal elements of the data estimation MSE matrix, i.e.,

$$\begin{aligned} \text{Obj.4} : \quad & f_{\text{M-Schur}}^{\text{Concave}}(d^2[\mathbf{L}]), \\ \text{with} \quad & \Phi_{\text{MSE}}^{\text{L}}(\mathbf{G}_A, \{\bar{\mathbf{F}}_k\}, \{\mathbf{Q}_k\}) = \mathbf{L}\mathbf{L}^H, \end{aligned} \quad (34)$$

the optimal solution of \mathbf{Q}_0 is given by [26]

$$\mathbf{Q}_{0,\text{opt}} = \mathbf{V}_1. \quad (35)$$

It is obvious that when the objective function is multiplicatively Schur-concave, the matrix version SNR is a diagonal matrix at the optimal solution of $\mathbf{Q}_{0,\text{opt}}$.

Based on the optimal solution of $\{\mathbf{Q}_{k,\text{opt}}\}_{k=0}^{K-1}$, the nonlinear transceiver optimization problem can be rewritten as

$$\begin{aligned} \min_{\mathbf{G}_A, \{\bar{\mathbf{F}}_k\}} \quad & f_{\text{NL}}\left(\left\{\lambda\left\{\bar{\mathbf{F}}_k^H \widehat{\mathbf{H}}_k^H \mathbf{K}_{\mathbf{n}_k}^{-1} \widehat{\mathbf{H}}_k \bar{\mathbf{F}}_k\right\}\right\}\right), \\ \text{s.t.} \quad & \text{Tr}(\bar{\mathbf{F}}_k \bar{\mathbf{F}}_k^H) \leq P_k, \\ & \mathbf{F}_{\text{AL},k} \in \mathcal{F}_{\text{PL},k}, \mathbf{F}_{\text{AR},k} \in \mathcal{F}_{\text{PR},k}, \mathbf{G}_A \in \mathcal{F}_G. \end{aligned} \quad (36)$$

In a nutshell, for linear transceiver optimization and nonlinear transceiver optimization, the optimal solution is a Pareto optimal solution of the following optimization problem

$$\begin{aligned} \max_{\mathbf{G}_A, \{\bar{\mathbf{F}}_k\}} \quad & \left\{\lambda\left\{\bar{\mathbf{F}}_k^H \widehat{\mathbf{H}}_k^H \mathbf{K}_{\mathbf{n}_k}^{-1} \widehat{\mathbf{H}}_k \bar{\mathbf{F}}_k\right\}\right\}, \\ \text{s.t.} \quad & \text{Tr}(\bar{\mathbf{F}}_k \bar{\mathbf{F}}_k^H) \leq P_k, \\ & \mathbf{F}_{\text{AL},k} \in \mathcal{F}_{\text{PL},k}, \mathbf{F}_{\text{AR},k} \in \mathcal{F}_{\text{PR},k}, \mathbf{G}_A \in \mathcal{F}_G. \end{aligned} \quad (37)$$

Therefore, it is definitely true that the common structures of all the Pareto optimal solutions of the above vector optimization problem are the structures of the optimal solutions of our linear transceiver optimization problem and nonlinear transceiver optimization problem. In the following, we will derive the

optimal structures of the Pareto optimal solutions. Since for multi-hop AF MIMO communications, the hybrid transceiver optimizations are different in the first hop, the intermediate hops, and the final hop, we will investigate these hybrid transceiver optimizations case by case.

V. OPTIMAL STRUCTURES OF HYBRID TRANSCEIVERS

A. First Hop

The first-hop communication occurs between the source, node 0, and the first relay, node 1. By defining

$$\bar{\mathbf{F}}_{D,1} = \mathbf{F}_{D,1} \mathbf{R}_{\mathbf{x}_0}^{\frac{1}{2}}, \quad (38)$$

the vector optimization problem (37) for the first hop can be expressed in the following form

$$\begin{aligned} \max_{\bar{\mathbf{F}}_1} \quad & \lambda \left\{ \bar{\mathbf{F}}_{D,1}^H \mathbf{F}_{AL,1}^H \widehat{\mathbf{H}}_1^H \mathbf{K}_{n_1}^{-1} \widehat{\mathbf{H}}_1 \mathbf{F}_{AL,1} \bar{\mathbf{F}}_{D,1} \right\}, \\ \text{s.t.} \quad & \text{Tr}(\mathbf{F}_{AL,1} \bar{\mathbf{F}}_{D,1} \bar{\mathbf{F}}_{D,1}^H \mathbf{F}_{AL,1}^H) \leq P_1, \\ & \mathbf{F}_{AL,1} \in \mathcal{F}_{PL,1}. \end{aligned} \quad (39)$$

Noting the equivalent noise covariance matrix in the first hop

$$\mathbf{K}_{n_1} = (\sigma_{n_1}^2 + \text{Tr}(\mathbf{F}_{AL,1} \bar{\mathbf{F}}_{D,1} \bar{\mathbf{F}}_{D,1}^H \mathbf{F}_{AL,1}^H \Psi_1)) \mathbf{I} \triangleq \eta_1 \mathbf{I}, \quad (40)$$

it is obvious that the forward matrix optimization in the first hop is challenging to solve, and some reformulations are needed.

Note that the following power constraint

$$\text{Tr}(\mathbf{F}_{AL,1} \bar{\mathbf{F}}_{D,1} \bar{\mathbf{F}}_{D,1}^H \mathbf{F}_{AL,1}^H) \leq P_1 \quad (41)$$

is equivalent to the following one

$$\frac{\text{Tr}((\sigma_{n_1}^2 \mathbf{I} + P_1 \Psi_1) \mathbf{F}_{AL,1} \bar{\mathbf{F}}_{D,1} \bar{\mathbf{F}}_{D,1}^H \mathbf{F}_{AL,1}^H)}{\eta_1} \leq P_1. \quad (42)$$

Hence the optimization problem (39) is equivalent to

$$\begin{aligned} \max_{\bar{\mathbf{F}}_1} \quad & \lambda \left\{ \bar{\mathbf{F}}_{D,1}^H \mathbf{F}_{AL,1}^H \widehat{\mathbf{H}}_1^H \mathbf{K}_{n_1}^{-1} \widehat{\mathbf{H}}_1 \mathbf{F}_{AL,1} \bar{\mathbf{F}}_{D,1} \right\}, \\ \text{s.t.} \quad & \frac{\text{Tr}((\sigma_{n_1}^2 \mathbf{I} + P_1 \Psi_1) \mathbf{F}_{AL,1} \bar{\mathbf{F}}_{D,1} \bar{\mathbf{F}}_{D,1}^H \mathbf{F}_{AL,1}^H)}{\eta_1} \leq P_1, \\ & \mathbf{F}_{AL,1} \in \mathcal{F}_{PL,1}. \end{aligned} \quad (43)$$

By defining the following auxiliary variables

$$\tilde{\mathbf{F}}_{D,1} = \eta_1^{-\frac{1}{2}} \left(\mathbf{F}_{AL,1}^H (\sigma_{n_1}^2 \mathbf{I} + P_1 \Psi_1) \mathbf{F}_{AL,1} \right)^{\frac{1}{2}} \bar{\mathbf{F}}_{D,1}, \quad (44)$$

$$\mathbf{\Pi}_1 = (\sigma_{n_1}^2 \mathbf{I} + P_1 \Psi_1)^{\frac{1}{2}} \mathbf{F}_{AL,1} (\mathbf{F}_{AL,1}^H (\sigma_{n_1}^2 \mathbf{I} + P_1 \Psi_1) \mathbf{F}_{AL,1})^{-\frac{1}{2}}, \quad (45)$$

the vector optimization problem (43) can be rewritten in the following form

$$\begin{aligned} \max_{\bar{\mathbf{F}}_1} \quad & \lambda \left\{ \tilde{\mathbf{F}}_{D,1}^H \mathbf{\Pi}_1^H (\sigma_{n_1} \mathbf{I} + P_1 \Psi_1)^{-\frac{1}{2}} \widehat{\mathbf{H}}_1^H \right. \\ & \left. \times \widehat{\mathbf{H}}_1 (\sigma_{n_1} \mathbf{I} + P_1 \Psi_1)^{-\frac{1}{2}} \mathbf{\Pi}_1 \tilde{\mathbf{F}}_{D,1} \right\}, \\ \text{s.t.} \quad & \text{Tr}(\tilde{\mathbf{F}}_{D,1} \tilde{\mathbf{F}}_{D,1}^H) \leq P_1, \\ & \mathbf{F}_{AL,1} \in \mathcal{F}_{PL,1}, \end{aligned} \quad (46)$$

which is equivalent to the following matrix-monotonic optimization problem

$$\begin{aligned} \max_{\bar{\mathbf{F}}_1} \quad & \tilde{\mathbf{F}}_{D,1}^H \mathbf{\Pi}_1^H (\sigma_{n_1} \mathbf{I} + P_1 \Psi_1)^{-\frac{1}{2}} \widehat{\mathbf{H}}_1^H \\ & \times \widehat{\mathbf{H}}_1 (\sigma_{n_1} \mathbf{I} + P_1 \Psi_1)^{-\frac{1}{2}} \mathbf{\Pi}_1 \tilde{\mathbf{F}}_{D,1}, \\ \text{s.t.} \quad & \text{Tr}(\tilde{\mathbf{F}}_{D,1} \tilde{\mathbf{F}}_{D,1}^H) \leq P_1, \\ & \mathbf{F}_{AL,1} \in \mathcal{F}_{PL,1}. \end{aligned} \quad (47)$$

From (45), it is obvious that $\mathbf{\Pi}_1$ is determined by the analog transmit precoder $\mathbf{F}_{AL,1}$ and the nonzero singular values of $\mathbf{\Pi}_1$ are all ones. In other words, we only need to analyze the SVD unitary matrices of $\mathbf{\Pi}_1$. Furthermore, in the optimization problem (47), the constraint is unitary invariant to the digital forward matrix $\tilde{\mathbf{F}}_{D,1}$. This means that we only need to analyze the left SVD unitary matrix of $\mathbf{\Pi}_1$, which is equivalent to the left SVD unitary matrix of $(\sigma_{n_1}^2 \mathbf{I} + P_1 \Psi_1)^{\frac{1}{2}} \mathbf{F}_{AL,1}$. Then the following conclusion obviously holds.

Conclusion 2 The singular values of $(\sigma_{n_1}^2 \mathbf{I} + P_1 \Psi_1)^{\frac{1}{2}} \mathbf{F}_{AL,1}$ do not affect the system performance. The left eigenvectors of the SVD for $(\sigma_{n_1}^2 \mathbf{I} + P_1 \Psi_1)^{\frac{1}{2}} \mathbf{F}_{AL,1}$ have the maximum inner product with respect to the eigenvectors $\mathbf{V}_{\mathcal{H}_1}$, defined by the following SVD

$$\widehat{\mathbf{H}}_1 (\sigma_{n_1}^2 \mathbf{I} + P_1 \Psi_1)^{-\frac{1}{2}} = \mathbf{U}_{\mathcal{H}_1} \mathbf{\Lambda}_{\mathcal{H}_1} \mathbf{V}_{\mathcal{H}_1}^H \text{ with } \mathbf{\Lambda}_{\mathcal{H}_1} \searrow. \quad (48)$$

The optimal structure of $\tilde{\mathbf{F}}_{D,1}$ is readily derived in the following conclusion [4], [5].

Conclusion 3 Based on the SVD

$$\widehat{\mathbf{H}}_1 (\sigma_{n_1}^2 \mathbf{I} + P_1 \Psi_1)^{-\frac{1}{2}} \mathbf{\Pi}_1 = \mathbf{U}_{\mathbf{\Pi},1} \mathbf{\Lambda}_{\mathbf{\Pi},1} \mathbf{V}_{\mathbf{\Pi},1}^H \text{ with } \mathbf{\Lambda}_{\mathbf{\Pi},1} \searrow \quad (49)$$

for given $\mathbf{F}_{AL,1}$, all the Pareto optimal $\tilde{\mathbf{F}}_{D,1}$ of the optimization problem (47) satisfy the following structure

$$\tilde{\mathbf{F}}_{D,1} = \mathbf{V}_{\mathbf{\Pi},1} \mathbf{\Lambda}_{\tilde{\mathbf{F}}_{D,1}} \mathbf{U}_{\text{Arb}}^H, \quad (50)$$

where $\mathbf{\Lambda}_{\tilde{\mathbf{F}}_{D,1}}$ is a rectangular diagonal matrix, and \mathbf{U}_{Arb} is an arbitrary right unitary matrix with proper dimension.

Based on Conclusion 3 and the definition (44), when the optimal $\tilde{\mathbf{F}}_{D,1}$ is given, the optimal $\bar{\mathbf{F}}_{D,1}$ is readily computed as

$$\bar{\mathbf{F}}_{D,1} = \sqrt{\frac{P_1}{\alpha_1}} \left(\mathbf{F}_{AL,1}^H (\sigma_{n_1}^2 \mathbf{I} + P_1 \Psi_1) \mathbf{F}_{AL,1} \right)^{-\frac{1}{2}} \tilde{\mathbf{F}}_{D,1}, \quad (51)$$

in which α_1 is given by

$$\begin{aligned} \alpha_1 = & \text{Tr} \left(\left(\mathbf{F}_{AL,1}^H (\sigma_{n_1}^2 \mathbf{I} + P_1 \Psi_1) \mathbf{F}_{AL,1} \right)^{-\frac{1}{2}} \mathbf{F}_{AL,1}^H \mathbf{F}_{AL,1} \right. \\ & \left. \times \left(\mathbf{F}_{AL,1}^H (\sigma_{n_1}^2 \mathbf{I} + P_1 \Psi_1) \mathbf{F}_{AL,1} \right)^{-\frac{1}{2}} \tilde{\mathbf{F}}_{D,1} \tilde{\mathbf{F}}_{D,1}^H \right). \end{aligned} \quad (52)$$

B. Intermediate Hops

First define

$$\bar{\mathbf{F}}_{AR,k} = \mathbf{F}_{AR,k} \mathbf{R}_{\mathbf{x}_{k-1}}^{\frac{1}{2}}, \quad 2 \leq k \leq K. \quad (53)$$

Then the optimal forwarding matrices in the intermediate hops, namely, the hops $2 \leq k \leq K-1$, are the Pareto optimal solutions of the following optimization

$$\begin{aligned} \max_{\bar{\mathbf{F}}_k} & \lambda \left\{ \bar{\mathbf{F}}_{\text{AR},k}^H \mathbf{F}_{\text{D},k}^H \mathbf{F}_{\text{AL},k}^H \widehat{\mathbf{H}}_k^H \mathbf{K}_{\mathbf{n}_k}^{-1} \widehat{\mathbf{H}}_k \mathbf{F}_{\text{AL},k} \mathbf{F}_{\text{D},k} \bar{\mathbf{F}}_{\text{AR},k} \right\}, \\ \text{s.t.} & \text{Tr}(\mathbf{F}_{\text{AL},k} \mathbf{F}_{\text{D},k} \bar{\mathbf{F}}_{\text{AR},k} \bar{\mathbf{F}}_{\text{AR},k}^H \mathbf{F}_{\text{D},k}^H \mathbf{F}_{\text{AL},k}^H) \leq P_k, \\ & \mathbf{F}_{\text{AL},k} \in \mathcal{F}_{\text{PL},k}, \mathbf{F}_{\text{AR},k} \in \mathcal{F}_{\text{PR},k}. \end{aligned} \quad (54)$$

Noting the equivalent noise covariance matrix

$$\begin{aligned} \mathbf{K}_{\mathbf{n}_k} &= \left(\sigma_{\mathbf{n}_k}^2 \mathbf{I} + \text{Tr}(\mathbf{F}_{\text{AL},k} \mathbf{F}_{\text{D},k} \bar{\mathbf{F}}_{\text{AR},k} \bar{\mathbf{F}}_{\text{AR},k}^H \mathbf{F}_{\text{D},k}^H \mathbf{F}_{\text{AL},k}^H \Psi_k) \right) \mathbf{I} \\ &\triangleq \eta_k \mathbf{I}, \end{aligned} \quad (55)$$

the power constraint

$$\text{Tr}(\mathbf{F}_{\text{AL},k} \mathbf{F}_{\text{D},k} \bar{\mathbf{F}}_{\text{AR},k} \bar{\mathbf{F}}_{\text{AR},k}^H \mathbf{F}_{\text{D},k}^H \mathbf{F}_{\text{AL},k}^H) \leq P_k \quad (56)$$

is equivalent to the following one

$$\frac{\text{Tr}((\sigma_{\mathbf{n}_k}^2 \mathbf{I} + P_k \Psi_k) \mathbf{F}_{\text{AL},k} \mathbf{F}_{\text{D},k} \bar{\mathbf{F}}_{\text{AR},k} \bar{\mathbf{F}}_{\text{AR},k}^H \mathbf{F}_{\text{D},k}^H \mathbf{F}_{\text{AL},k}^H)}{\eta_k} \leq P_k. \quad (57)$$

As a result, after replacing the original constraint, the optimization problem (54) is equivalent to the following one

$$\begin{aligned} \max_{\bar{\mathbf{F}}_k} & \lambda \left\{ \bar{\mathbf{F}}_{\text{AR},k}^H \mathbf{F}_{\text{D},k}^H \mathbf{F}_{\text{AL},k}^H \widehat{\mathbf{H}}_k^H \mathbf{K}_{\mathbf{n}_k}^{-1} \widehat{\mathbf{H}}_k \mathbf{F}_{\text{AL},k} \mathbf{F}_{\text{D},k} \bar{\mathbf{F}}_{\text{AR},k} \right\}, \\ \text{s.t.} & \frac{\text{Tr}((\sigma_{\mathbf{n}_k}^2 \mathbf{I} + P_k \Psi_k) \mathbf{F}_{\text{AL},k} \mathbf{F}_{\text{D},k} \bar{\mathbf{F}}_{\text{AR},k} \bar{\mathbf{F}}_{\text{AR},k}^H \mathbf{F}_{\text{D},k}^H \mathbf{F}_{\text{AL},k}^H)}{\eta_k} \leq P_k, \\ & \mathbf{F}_{\text{AL},k} \in \mathcal{F}_{\text{PL},k}, \mathbf{F}_{\text{AR},k} \in \mathcal{F}_{\text{PR},k}. \end{aligned} \quad (58)$$

By defining the following auxiliary variables

$$\begin{aligned} \tilde{\mathbf{F}}_{\text{D},k} &= \eta_k^{-\frac{1}{2}} \left(\mathbf{F}_{\text{AL},k}^H (\sigma_{\mathbf{n}_k}^2 \mathbf{I} + P_k \Psi_k) \mathbf{F}_{\text{AL},k} \right)^{\frac{1}{2}} \mathbf{F}_{\text{D},k} \\ &\quad \times (\bar{\mathbf{F}}_{\text{AR},k} \bar{\mathbf{F}}_{\text{AR},k}^H)^{\frac{1}{2}} \tilde{\mathbf{U}}_k^H, \end{aligned} \quad (59)$$

$$\Pi_{\text{R},k} = (\bar{\mathbf{F}}_{\text{AR},k} \bar{\mathbf{F}}_{\text{AR},k}^H)^{-\frac{1}{2}} \bar{\mathbf{F}}_{\text{AR},k}, \quad (60)$$

$$\begin{aligned} \Pi_{\text{L},k} &= (\sigma_{\mathbf{n}_k}^2 \mathbf{I} + P_k \Psi_k)^{\frac{1}{2}} \mathbf{F}_{\text{AL},k} \\ &\quad \times \left(\mathbf{F}_{\text{AL},k}^H (\sigma_{\mathbf{n}_k}^2 \mathbf{I} + P_k \Psi_k) \mathbf{F}_{\text{AL},k} \right)^{-\frac{1}{2}}, \end{aligned} \quad (61)$$

where $\tilde{\mathbf{U}}_k$ is a left unitary matrix of appropriate dimension yet to be determined, the optimization problem (58) can be reformulated into

$$\begin{aligned} \max_{\bar{\mathbf{F}}_k} & \lambda \left\{ \Pi_{\text{R},k}^H \tilde{\mathbf{U}}_k^H \tilde{\mathbf{F}}_{\text{D},k}^H \Pi_{\text{L},k}^H (\sigma_{\mathbf{n}_k}^2 \mathbf{I} + P_k \Psi_k)^{-\frac{1}{2}} \widehat{\mathbf{H}}_k^H \widehat{\mathbf{H}}_k \right. \\ & \quad \left. \times (\sigma_{\mathbf{n}_k}^2 \mathbf{I} + P_k \Psi_k)^{-\frac{1}{2}} \Pi_{\text{L},k} \tilde{\mathbf{F}}_{\text{D},k} \tilde{\mathbf{U}}_k \Pi_{\text{R},k} \right\}, \\ \text{s.t.} & \text{Tr}(\tilde{\mathbf{F}}_{\text{D},k} \tilde{\mathbf{F}}_{\text{D},k}^H) \leq P_k, \\ & \mathbf{F}_{\text{AL},k} \in \mathcal{F}_{\text{PL},k}, \mathbf{F}_{\text{AR},k} \in \mathcal{F}_{\text{PR},k}. \end{aligned} \quad (62)$$

Similar to point-to-point MIMO systems [27], we have the following two conclusions.

Conclusion 4 Based on the definition of $\Pi_{\text{R},k}$ in (60), it can be concluded that the singular values of $\mathbf{F}_{\text{AR},k}$ do not affect the system performance. The right singular vectors of the

optimal $\bar{\mathbf{F}}_{\text{AR},k}$ correspond to the left singular vectors of the preceding-hop channel, i.e., $\mathbf{U}_{\mathbf{H}_k}^H$.

Conclusion 5 Based on the SVDs

$$\widehat{\mathbf{H}}_k (\sigma_{\mathbf{n}_k}^2 \mathbf{I} + P_k \Psi_k)^{-\frac{1}{2}} \Pi_{\text{L},k} \tilde{\mathbf{F}}_{\text{D},k} = \tilde{\mathbf{U}}_k \tilde{\Lambda}_k \tilde{\mathbf{V}}_k^H \text{ with } \tilde{\Lambda}_k \searrow, \quad (63)$$

$$\Pi_{\text{R},k} = \mathbf{U}_{\Pi_{\text{R},k}} \Lambda_{\Pi_{\text{R},k}} \mathbf{V}_{\Pi_{\text{R},k}}^H \text{ with } \Lambda_{\Pi_{\text{R},k}} \searrow, \quad (64)$$

the optimal $\tilde{\mathbf{U}}_k$ equals to

$$\tilde{\mathbf{U}}_{k,\text{opt}} = \tilde{\mathbf{V}}_k \mathbf{U}_{\Pi_{\text{R},k}}^H. \quad (65)$$

Based on Conclusions 4 and 5, the optimization problem (62) is equivalent to the following much simpler one

$$\begin{aligned} \max_{\bar{\mathbf{F}}_k} & \lambda \left\{ \tilde{\mathbf{F}}_{\text{D},k}^H \Pi_{\text{L},k}^H (\sigma_{\mathbf{n}_k}^2 \mathbf{I} + P_k \Psi_k)^{-\frac{1}{2}} \widehat{\mathbf{H}}_k^H \widehat{\mathbf{H}}_k \right. \\ & \quad \left. \times (\sigma_{\mathbf{n}_k}^2 \mathbf{I} + P_k \Psi_k)^{-\frac{1}{2}} \Pi_{\text{L},k} \tilde{\mathbf{F}}_{\text{D},k} \right\}, \\ \text{s.t.} & \text{Tr}(\tilde{\mathbf{F}}_{\text{D},k} \tilde{\mathbf{F}}_{\text{D},k}^H) \leq P_k, \\ & \mathbf{F}_{\text{AL},k} \in \mathcal{F}_{\text{PL},k}, \mathbf{F}_{\text{AR},k} \in \mathcal{F}_{\text{PR},k}, \end{aligned} \quad (66)$$

which is equivalent to the following matrix monotonic optimization problem

$$\begin{aligned} \max_{\bar{\mathbf{F}}_k} & \tilde{\mathbf{F}}_{\text{D},k}^H \Pi_{\text{L},k}^H (\sigma_{\mathbf{n}_k}^2 \mathbf{I} + P_k \Psi_k)^{-\frac{1}{2}} \widehat{\mathbf{H}}_k^H \widehat{\mathbf{H}}_k \\ & \quad \times (\sigma_{\mathbf{n}_k}^2 \mathbf{I} + P_k \Psi_k)^{-\frac{1}{2}} \Pi_{\text{L},k} \tilde{\mathbf{F}}_{\text{D},k}, \\ \text{s.t.} & \text{Tr}(\tilde{\mathbf{F}}_{\text{D},k} \tilde{\mathbf{F}}_{\text{D},k}^H) \leq P_k, \\ & \mathbf{F}_{\text{AL},k} \in \mathcal{F}_{\text{PL},k}, \mathbf{F}_{\text{AR},k} \in \mathcal{F}_{\text{PR},k}. \end{aligned} \quad (67)$$

Similar to the matrix monotonic optimization (47), we can readily obtain the optimal solution of (67).

Conclusion 6 The singular values of $(\sigma_{\mathbf{n}_k}^2 \mathbf{I} + P_k \Psi_k)^{\frac{1}{2}} \mathbf{F}_{\text{AL},k}$ do not affect the system performance. The left eigenvectors of the SVD for $(\sigma_{\mathbf{n}_k}^2 \mathbf{I} + P_k \Psi_k)^{\frac{1}{2}} \mathbf{F}_{\text{AL},k}$ have the maximum inner product with respect to the eigenvectors $\mathbf{V}_{\mathbf{H}_k}$ defined by the following SVD

$$\widehat{\mathbf{H}}_k (\sigma_{\mathbf{n}_k}^2 \mathbf{I} + P_k \Psi_k)^{-\frac{1}{2}} = \mathbf{U}_{\mathbf{H}_k} \Lambda_{\mathbf{H}_k} \mathbf{V}_{\mathbf{H}_k}^H \text{ with } \Lambda_{\mathbf{H}_k} \searrow. \quad (68)$$

Conclusion 7 Based on the SVD

$$\widehat{\mathbf{H}}_k (\sigma_{\mathbf{n}_k}^2 \mathbf{I} + P_k \Psi_k)^{-\frac{1}{2}} \Pi_{\text{L},k} = \mathbf{U}_{\Pi_{\text{L},k}} \Lambda_{\Pi_{\text{L},k}} \mathbf{V}_{\Pi_{\text{L},k}}^H \text{ with } \Lambda_{\Pi_{\text{L},k}} \searrow, \quad (69)$$

for given $\mathbf{F}_{\text{AL},k}$, all the Pareto optimal $\tilde{\mathbf{F}}_{\text{D},k}$ of the optimization problem (67) satisfy the following structure

$$\tilde{\mathbf{F}}_{\text{D},k} = \mathbf{V}_{\Pi_{\text{L},k}} \Lambda_{\tilde{\mathbf{F}}_{\text{D},k}} \mathbf{U}_{\text{Arb}}^H, \quad (70)$$

where $\Lambda_{\tilde{\mathbf{F}}_{\text{D},k}}$ is a rectangular diagonal matrix.

Based on Conclusion 7 and the definition (59), after computing the optimal $\tilde{\mathbf{F}}_{\text{D},k}$, the optimal $\mathbf{F}_{\text{D},k}$ is given by

$$\begin{aligned} \mathbf{F}_{\text{D},k} &= \sqrt{\frac{P_k}{\alpha_k}} \left(\mathbf{F}_{\text{AL},k}^H (\sigma_{\mathbf{n}_k}^2 \mathbf{I} + P_k \Psi_k) \mathbf{F}_{\text{AL},k} \right)^{-\frac{1}{2}} \\ &\quad \times \tilde{\mathbf{F}}_{\text{D},k} \tilde{\mathbf{U}}_k (\bar{\mathbf{F}}_{\text{AR},k} \bar{\mathbf{F}}_{\text{AR},k}^H)^{-\frac{1}{2}}, \end{aligned} \quad (71)$$

where

$$\begin{aligned} \alpha_k &= \text{Tr} \left(\left(\mathbf{F}_{\text{AL},k}^H (\sigma_{\mathbf{n}_k}^2 \mathbf{I} + P_k \Psi_k) \mathbf{F}_{\text{AL},k} \right)^{-\frac{1}{2}} \mathbf{F}_{\text{AL},k}^H \mathbf{F}_{\text{AL},k} \right. \\ &\quad \left. \times \left(\mathbf{F}_{\text{AL},k}^H (\sigma_{\mathbf{n}_k}^2 \mathbf{I} + P_k \Psi_k) \mathbf{F}_{\text{AL},k} \right)^{-\frac{1}{2}} \tilde{\mathbf{F}}_{\text{D},k} \tilde{\mathbf{F}}_{\text{D},k}^H \right). \end{aligned} \quad (72)$$

C. Final Hop

By noting the definition (53), the forwarding matrix optimization problem (37) for the final K th hop becomes

$$\begin{aligned} \max_{\mathbf{G}_A, \mathbf{F}_K} & \lambda \left\{ \bar{\mathbf{F}}_{AR,K}^H \mathbf{F}_{D,K}^H \mathbf{F}_{AL,K}^H \widehat{\mathbf{H}}_K^H \mathbf{G}_A^H \mathbf{K}_{n_K}^{-1} \right. \\ & \quad \left. \times \mathbf{G}_A \widehat{\mathbf{H}}_K \mathbf{F}_{AL,K} \mathbf{F}_{D,K} \bar{\mathbf{F}}_{AR,K} \right\}, \\ \text{s.t.} & \quad \text{Tr}(\mathbf{F}_{AL,K} \mathbf{F}_{D,K} \bar{\mathbf{F}}_{AR,K} \bar{\mathbf{F}}_{AR,K}^H \mathbf{F}_{D,K}^H \mathbf{F}_{AL,K}^H) \leq P_K, \\ & \quad \mathbf{F}_{AL,K} \in \mathcal{F}_{PL,K}, \mathbf{F}_{AR,K} \in \mathcal{F}_{PR,K}, \mathbf{G}_A \in \mathcal{F}_G, \end{aligned} \quad (73)$$

where the equivalent noise covariance matrix is given by

$$\begin{aligned} \mathbf{K}_{n_K} = & \mathbf{G}_A \left(\left(\sigma_{n_K}^2 + \text{Tr}(\mathbf{F}_{AL,K} \mathbf{F}_{D,K} \bar{\mathbf{F}}_{AR,K} \bar{\mathbf{F}}_{AR,K}^H \mathbf{F}_{D,K}^H \mathbf{F}_{AL,K}^H) \right. \right. \\ & \quad \left. \left. \times \mathbf{F}_{AL,K}^H \Psi_K \right) \mathbf{I} \right) \mathbf{G}_A^H \triangleq \eta_K \mathbf{G}_A \mathbf{G}_A^H. \end{aligned} \quad (74)$$

Clearly, the power constraint in (73), namely,

$$\text{Tr}(\mathbf{F}_{AL,K} \mathbf{F}_{D,K} \bar{\mathbf{F}}_{AR,K} \bar{\mathbf{F}}_{AR,K}^H \mathbf{F}_{D,K}^H \mathbf{F}_{AL,K}^H) \leq P_K \quad (75)$$

is equivalent to the following one

$$\begin{aligned} & \frac{\text{Tr} \left((\sigma_{n_K}^2 \mathbf{I} + P_K \Psi_K) \mathbf{F}_{AL,K} \mathbf{F}_{D,K} \bar{\mathbf{F}}_{AR,K} \bar{\mathbf{F}}_{AR,K}^H \mathbf{F}_{D,K}^H \mathbf{F}_{AL,K}^H \right)}{\eta_K} \\ & \leq P_K. \end{aligned} \quad (76)$$

By defining the following auxiliary variables

$$\begin{aligned} \tilde{\mathbf{F}}_{D,K} = & \eta_K^{-\frac{1}{2}} \left(\mathbf{F}_{AL,K}^H (\sigma_{n_K}^2 \mathbf{I} + P_K \Psi_K) \mathbf{F}_{AL,K} \right)^{\frac{1}{2}} \mathbf{F}_{D,K} \\ & \times \left(\bar{\mathbf{F}}_{AR,K} \bar{\mathbf{F}}_{AR,K}^H \right)^{\frac{1}{2}} \tilde{\mathbf{U}}_K^H, \end{aligned} \quad (77)$$

$$\mathbf{\Pi}_{R,K} = \left(\bar{\mathbf{F}}_{AR,K} \bar{\mathbf{F}}_{AR,K}^H \right)^{-\frac{1}{2}} \bar{\mathbf{F}}_{AR,K}, \quad (78)$$

$$\begin{aligned} \mathbf{\Pi}_{L,K} = & (\sigma_{n_K}^2 \mathbf{I} + P_K \Psi_K)^{\frac{1}{2}} \mathbf{F}_{AL,K} \left(\mathbf{F}_{AL,K}^H \right. \\ & \quad \left. \times (\sigma_{n_K}^2 \mathbf{I} + P_K \Psi_K) \mathbf{F}_{AL,K} \right)^{-\frac{1}{2}}, \end{aligned} \quad (79)$$

$$\mathbf{\Pi}_G = (\mathbf{G}_A \mathbf{G}_A^H)^{-\frac{1}{2}} \mathbf{G}_A, \quad (80)$$

where $\tilde{\mathbf{U}}_K$ is a left unitary matrix yet to be determined, the vector optimization problem (73) can be reformulated as

$$\begin{aligned} \max_{\mathbf{G}_A, \mathbf{F}_K} & \lambda \left\{ \mathbf{\Pi}_{R,K}^H \tilde{\mathbf{U}}_K^H \tilde{\mathbf{F}}_{D,K}^H \mathbf{\Pi}_{L,K}^H (\sigma_{n_K}^2 \mathbf{I} + P_K \Psi_K)^{-\frac{1}{2}} \widehat{\mathbf{H}}_K^H \mathbf{\Pi}_G^H \right. \\ & \quad \left. \times \mathbf{\Pi}_G \widehat{\mathbf{H}}_K (\sigma_{n_K}^2 \mathbf{I} + P_K \Psi_K)^{-\frac{1}{2}} \mathbf{\Pi}_{L,K} \tilde{\mathbf{F}}_{D,K} \tilde{\mathbf{U}}_K \mathbf{\Pi}_{R,K} \right\}, \\ \text{s.t.} & \quad \text{Tr}(\tilde{\mathbf{F}}_{D,K} \tilde{\mathbf{F}}_{D,K}^H) \leq P_K, \\ & \quad \mathbf{F}_{AL,K} \in \mathcal{F}_{PL,K}, \mathbf{F}_{AR,K} \in \mathcal{F}_{PR,K}, \mathbf{G}_A \in \mathcal{F}_G, \end{aligned} \quad (81)$$

Then we readily have the following two conclusions.

Conclusion 8 Based on the definition of $\mathbf{\Pi}_{R,K}$, it can be concluded that the singular values of $\bar{\mathbf{F}}_{AR,K}$ do not affect the system performance. The right singular vectors of the optimal $\bar{\mathbf{F}}_{AR,K}$ correspond to the left singular vectors of the preceding-hop channel, i.e., $\mathbf{U}_{\mathcal{H}_K}^H$.

Conclusion 9 Based on the SVDs

$$\widehat{\mathbf{H}}_K (\sigma_{n_K}^2 \mathbf{I} + P_K \Psi_K)^{-\frac{1}{2}} \mathbf{\Pi}_{L,K} \tilde{\mathbf{F}}_{D,K} = \tilde{\mathbf{U}}_K \tilde{\mathbf{\Lambda}}_K \tilde{\mathbf{V}}_K^H \text{ with } \tilde{\mathbf{\Lambda}}_K \searrow, \quad (82)$$

$$\mathbf{\Pi}_{R,K} = \mathbf{U}_{\mathbf{\Pi}_{R,K}} \mathbf{\Lambda}_{\mathbf{\Pi}_{R,K}} \mathbf{V}_{\mathbf{\Pi}_{R,K}}^H \text{ with } \mathbf{\Lambda}_{\mathbf{\Pi}_{R,K}} \searrow, \quad (83)$$

the optimal $\tilde{\mathbf{U}}_K$ is derived as

$$\tilde{\mathbf{U}}_{K,\text{opt}} = \tilde{\mathbf{V}}_K \mathbf{U}_{\mathbf{\Pi}_{R,K}}^H. \quad (84)$$

Based on Conclusions 8 and 9, the optimization problem (81) can be simplified into the following one

$$\begin{aligned} \max_{\mathbf{G}_A, \mathbf{F}_K} & \lambda \left\{ \tilde{\mathbf{F}}_{D,K}^H \mathbf{\Pi}_{L,K}^H (\sigma_{n_K}^2 \mathbf{I} + P_K \Psi_K)^{-\frac{1}{2}} \widehat{\mathbf{H}}_K^H \mathbf{\Pi}_G^H \right. \\ & \quad \left. \times \mathbf{\Pi}_G \widehat{\mathbf{H}}_K (\sigma_{n_K}^2 \mathbf{I} + P_K \Psi_K)^{-\frac{1}{2}} \mathbf{\Pi}_{L,K} \tilde{\mathbf{F}}_{D,K} \right\}, \\ \text{s.t.} & \quad \text{Tr}(\tilde{\mathbf{F}}_{D,K} \tilde{\mathbf{F}}_{D,K}^H) \leq P_K, \\ & \quad \mathbf{F}_{AL,K} \in \mathcal{F}_{PL,K}, \mathbf{F}_{AR,K} \in \mathcal{F}_{PR,K}, \mathbf{G}_A \in \mathcal{F}_G, \end{aligned} \quad (85)$$

The optimization (85) is equivalent to the following matrix monotonic optimization problem

$$\begin{aligned} \max_{\mathbf{G}_A, \mathbf{F}_K} & \tilde{\mathbf{F}}_{D,K}^H \mathbf{\Pi}_{L,K}^H (\sigma_{n_K}^2 \mathbf{I} + P_K \Psi_K)^{-\frac{1}{2}} \widehat{\mathbf{H}}_K^H \mathbf{\Pi}_G^H \\ & \quad \times \mathbf{\Pi}_G \widehat{\mathbf{H}}_K (\sigma_{n_K}^2 \mathbf{I} + P_K \Psi_K)^{-\frac{1}{2}} \mathbf{\Pi}_{L,K} \tilde{\mathbf{F}}_{D,K}, \\ \text{s.t.} & \quad \text{Tr}(\tilde{\mathbf{F}}_{D,K} \tilde{\mathbf{F}}_{D,K}^H) \leq P_K, \\ & \quad \mathbf{F}_{AL,K} \in \mathcal{F}_{PL,K}, \mathbf{F}_{AR,K} \in \mathcal{F}_{PR,K}, \mathbf{G}_A \in \mathcal{F}_G, \end{aligned} \quad (86)$$

and we readily have the following three conclusions.

Conclusion 10 The singular values of the matrix $(\sigma_{n_K}^2 \mathbf{I} + P_K \Psi_K)^{\frac{1}{2}} \mathbf{F}_{AL,K}$ do not affect the system performance. The left eigenvectors of the SVD for $(\sigma_{n_K}^2 \mathbf{I} + P_K \Psi_K)^{\frac{1}{2}} \mathbf{F}_{AL,K}$ have the maximum inner product with respect to the eigenvectors $\mathbf{V}_{\mathcal{H}_K}$ defined by the following SVD

$$\widehat{\mathbf{H}}_K (\sigma_{n_K}^2 \mathbf{I} + P_K \Psi_K)^{-\frac{1}{2}} = \mathbf{U}_{\mathcal{H}_K} \mathbf{\Lambda}_{\mathcal{H}_K} \mathbf{V}_{\mathcal{H}_K}^H \text{ with } \mathbf{\Lambda}_{\mathcal{H}_K} \searrow. \quad (87)$$

Conclusion 11 The singular values of \mathbf{G}_A do not affect the system performance. The right eigenvectors of the SVD for \mathbf{G}_A have the maximum inner product with respect to the eigenvectors $\mathbf{U}_{\mathcal{H}_K}$.

Conclusion 12 Based on the SVD

$$\begin{aligned} \mathbf{\Pi}_G \widehat{\mathbf{H}}_K (\sigma_{n_K}^2 \mathbf{I} + P_K \Psi_K)^{-\frac{1}{2}} \mathbf{\Pi}_{L,K} = & \mathbf{U}_{\mathbf{\Pi},K} \mathbf{\Lambda}_{\mathbf{\Pi},K} \mathbf{V}_{\mathbf{\Pi},K}^H \\ \text{with } & \mathbf{\Lambda}_{\mathbf{\Pi},K} \searrow, \end{aligned} \quad (88)$$

for given $\mathbf{F}_{AL,K}$, all the Pareto optimal solutions $\tilde{\mathbf{F}}_{D,K}$ of the optimization problem (86) satisfy the following structure

$$\tilde{\mathbf{F}}_{D,K} = \mathbf{V}_{\mathbf{\Pi},K} \mathbf{\Lambda}_{\tilde{\mathbf{F}}_{D,K}} \mathbf{U}_{\text{Arb}}^H, \quad (89)$$

where $\mathbf{\Lambda}_{\tilde{\mathbf{F}}_{D,K}}$ is a rectangular diagonal matrix and \mathbf{U}_{Arb} is an arbitrary unitary matrix with a proper dimension.

Based on the definition (77), when the optimal $\tilde{\mathbf{F}}_{D,K}$ is given, the optimal $\mathbf{F}_{D,K}$ can be computed according to

$$\begin{aligned} \mathbf{F}_{D,K} = & \sqrt{\frac{P_K}{\alpha_K}} \left(\mathbf{F}_{AL,K}^H (\sigma_{n_K}^2 \mathbf{I} + P_K \Psi_K) \mathbf{F}_{AL,K} \right)^{-\frac{1}{2}} \\ & \times \tilde{\mathbf{F}}_{D,K} \tilde{\mathbf{U}}_K (\bar{\mathbf{F}}_{AR,K} \bar{\mathbf{F}}_{AR,K}^H)^{-\frac{1}{2}}, \end{aligned} \quad (90)$$

where α_K is given by

$$\begin{aligned} \alpha_K = & \text{Tr} \left(\left(\mathbf{F}_{AL,K}^H (\sigma_{n_K}^2 \mathbf{I} + P_K \Psi_K) \mathbf{F}_{AL,K} \right)^{-\frac{1}{2}} \mathbf{F}_{AL,K}^H \mathbf{F}_{AL,K} \right. \\ & \quad \left. \times \left(\mathbf{F}_{AL,K}^H (\sigma_{n_K}^2 \mathbf{I} + P_K \Psi_K) \mathbf{F}_{AL,K} \right)^{-\frac{1}{2}} \tilde{\mathbf{F}}_{D,K}^H \tilde{\mathbf{F}}_{D,K} \right). \end{aligned} \quad (91)$$

VI. OPTIMAL SOLUTIONS $\Lambda_{\tilde{F}_{D,k}}$

The optimal solutions $\Lambda_{\tilde{F}_{D,k}}$ for $1 \leq k \leq K$ in Conclusions 3, 7 and 12 are determined by the different performance metrics, correspondingly. Fortunately, for these performance metrics, the derivations are almost identical. Specifically, the optimal solutions of the diagonal elements of $\Lambda_{\tilde{F}_{D,k}}$ can be derived based the Karush-Kuhn-Tucker (KKT) conditions and the solutions are variants of the water-filling solutions. It is worth highlighting that similar content can be found in our previous paper [4], [26] on full digital multi-hop transceiver design. However, to make this paper self-contained, the optimal solution of $\Lambda_{\tilde{F}_{D,k}}$ for the capacity maximization and the sum MSE minimization will be briefly listed in the following part. From these two examples, a clear logic of digital beamforming designs for multi-hop AF MIMO relaying systems is revealed.

Based on Conclusions 2 to 12, when the capacity maximization problem for multi-hop AF MIMO relaying systems is considered, the digital beamformer optimization problem becomes

$$\begin{aligned} \min_{\{f_{k,i}\}} \quad & \sum_{i=1}^N \log \left(1 - \prod_{k=1}^K \frac{f_{k,i}^2 \lambda_{k,i}^2}{1 + f_{k,i}^2 \lambda_{k,i}^2} \right), \\ \text{s.t.} \quad & \sum_{i=1}^N f_{k,i}^2 \leq P_k, 1 \leq k \leq K, \end{aligned} \quad (92)$$

where the optimization variables $\{f_{k,i}\}$ are the diagonal elements of the diagonal matrix $\Lambda_{\tilde{F}_{D,k}}$, and the parameters $\{\lambda_{k,i}\}$ are the diagonal elements of the diagonal matrix $\Lambda_{\Pi,k}$. Similar to [4], an iterative water-filling algorithm can be used to solve this problem. In each iteration, based on the KKT conditions, the water-filling solution can be derived to be [4]

$$f_{k,i}^2 = \frac{1}{\lambda_{k,i}^2} \left(\frac{c_{k,i} - 2 + \sqrt{c_{k,i}^2 + \frac{4(1-c_{k,i})c_{k,i}\lambda_{k,i}^2}{\nu_k}}}{2(1-c_{k,i})} \right)^+, \quad (93)$$

where ν_k is the Lagrange multiplier corresponding to the transmit power constraint in the k th hop, which can be simply computed using classic bisection search [4], while $c_{k,i}$ is defined as follows

$$c_{k,i} = \prod_{l \neq k} \frac{f_{l,i}^2 \lambda_{l,i}^2}{1 + f_{l,i}^2 \lambda_{l,i}^2}. \quad (94)$$

On the other hand, for the weighted MSE minimization of multi-hop AF MIMO relaying systems, the optimization of digital beamformer can be transferred into the following one

$$\begin{aligned} \min_{\{f_{k,i}\}} \quad & \sum_{i=1}^N w_i \left(1 - \frac{\prod_{k=1}^K f_{k,i}^2 \lambda_{k,i}^2}{1 + \prod_{k=1}^K f_{k,i}^2 \lambda_{k,i}^2} \right), \\ \text{s.t.} \quad & \sum_{i=1}^N f_{k,i}^2 \leq P_k, 1 \leq k \leq K, \end{aligned} \quad (95)$$

where w_i for $1 \leq i \leq N$ are the weighting factors. Similarly, the iterative water-filling algorithm can also be used [4]. In each iteration, based on the KKT conditions, the water-filling solution can be derived to be [4]

$$f_{k,i}^2 = \left(\sqrt{\frac{w_i c_{k,i}}{\nu_k \lambda_{k,i}^2}} - \frac{1}{\lambda_{k,i}^2} \right)^+, \quad (96)$$

where ν_k is the Lagrange multiplier corresponding to the transmit power constraint in the k th hop, and $c_{k,i}$ is the same as given in (94).

At the end of this section, we would like to emphasize again that for other performance metrics, the derivation procedures are exactly the same as those presented above for the capacity maximization and the MSE minimization, and the resultant solutions are also variants of water-filling solutions. Based on these solutions, it can be concluded that the remaining task for hybrid transceiver optimizations of multi-hop AF MIMO communications is how to design analog transceivers based on the derived optimal structures.

VII. ANALOG TRANSCEIVER OPTIMIZATIONS

In the previous sections, the optimal structures of the hybrid transceivers for multi-hop communications are derived. However, due to the physical limitations imposed on the analog transceivers, the processing factors corresponding to individual analog antenna elements have unit modulus. Thus, it is challenging to design analog transceivers directly based on the derived optimal structures. In addition, for multi-hop AF MIMO relaying systems, the analog beamforming should be low complexity. This is the focus of this section.

A. Analog Transmit Precoder Design

From Section V, it can be seen that the auxiliary variable of the beamformer at the k th relay has the following form

$$\Pi_{L,k} = D_k F_{AL,k} (F_{AL,k}^H D_k^H D_k F_{AL,k})^{-\frac{1}{2}}, 1 \leq k \leq K, \quad (97)$$

where D_k is any invertible matrix with appropriate dimension, and $F_{AL,k}$ is the analog transmit precoder to be designed. It is interesting to know that (97) is actually a general form of analog beamformer design problem and thus can be utilized to other beamformer design situations. It is also worth noting that only the left singular matrix of $\Pi_{L,k}$, which is exactly the left singular matrix of $D_k F_{AL,k}$, accounts for the system performance. This means that given the SVD

$$D_k F_{AL,k} = U_{L,k} \Sigma_{L,k} V_{L,k}^H, \quad (98)$$

$U_{L,k}$ is the only part that is needed in the designing process.

It is instinctive that we could use the angle matrix of the desired value of $\Pi_{L,k}$, namely, $V_{\mathbf{H}_k}$, to compose the analog beamformer, which is denoted as $\mathcal{P}_{\mathcal{F}}(D_k^{-1} V_{\mathbf{H}_k})$. However, this operation is difficult to solve directly. An alternative design is to minimize the Frobenius norm of the error between the desired full digital solution and the unit-modulus beamformer. Different from the previous work, in this paper, a weighted norm is utilized to account for the varying influence of the different bases in the signal space. In this way, the associated optimization problem can be formulated as

$$\begin{aligned} \min_{\Sigma_{L,k}, V_{L,k}, F_{AL,k}} \quad & \left\| W_k^{\frac{1}{2}} (V_{\mathbf{H}_k} \Sigma_{L,k} V_{L,k}^H - D_k F_{AL,k}) \right\|_F^2, \\ \text{s.t.} \quad & V_{L,k} \in \mathcal{U}, F_{AL,k} \in \mathcal{F}_{PL,k}, \\ & \Sigma_{L,k} = \text{diag}\{\sigma_{L,1}, \dots, \sigma_{L,K}\}, \end{aligned} \quad (99)$$

where $\mathcal{U} = \{U | UU^H = U^H U = I, U \in \mathbb{C}^{n \times n}\}$ denotes the unitary matrix set, and the matrix set $\mathcal{F} = \{F | \|F\|_{i,j} =$

const, $\forall i, j$, while $\Sigma_{L,k}$ is a diagonal matrix, and K is the number of RF chains in the structure. Moreover, the weight matrix can be chosen as $\mathbf{W}_k = \mathbf{V}_{\mathcal{H}_k} \Lambda_{\mathbf{W}_k} \mathbf{V}_{\mathcal{H}_k}^H$ in which $\Lambda_{\mathbf{W}_k}$ is a diagonal matrix.

It is worth highlighting that there is no constraint imposed on the matrix variable $\Sigma_{L,k}$ in the optimization (99). As a result, the optimal $\Sigma_{L,k}$ can be derived in a closed-form as

$$\Sigma_{L,k} = \left(\text{diag} \{ d[\mathbf{V}_{\mathcal{H}_k}^H \mathbf{W}_k \mathbf{V}_{\mathcal{H}_k}] \} \right)^{-1} \times \Re \left(\text{diag} \{ d[\mathbf{V}_{L,k}^H \mathbf{F}_{AL,k}^H \mathbf{D}_k^H \mathbf{W}_k \mathbf{V}_{\mathcal{H}_k}] \} \right). \quad (100)$$

Given $\Sigma_{L,k}$, the next task is to find the optimal unitary matrix $\mathbf{V}_{L,k}$. For the following optimization problem

$$\begin{aligned} \min_{\mathbf{Q}} \quad & \|\mathbf{B}\mathbf{Q} - \mathbf{A}\|_F^2, \\ \text{s.t.} \quad & \mathbf{Q} \in \mathcal{U}, \end{aligned} \quad (101)$$

the optimal solution can be derived to be $\mathbf{Q} = \mathbf{U}\mathbf{V}^H$ [33], in which the unitary matrices \mathbf{U} and \mathbf{V} are defined based on the SVD $\mathbf{B}^H \mathbf{A} = \mathbf{U} \Sigma \mathbf{V}^H$. Therefore, for the optimization problem (99), the optimal $\mathbf{V}_{L,k}$ is given by

$$\mathbf{V}_{L,k} = \mathbf{U}_V^H \mathbf{V}_V, \quad (102)$$

where the unitary matrices \mathbf{U}_V and \mathbf{V}_V are defined based on the following SVD

$$(\mathbf{V}_{\mathcal{H}_k} \Sigma_{L,k})^H \mathbf{W}_k \mathbf{D}_k \mathbf{F}_{AL,k} = \mathbf{U}_V \Sigma_V \mathbf{V}_V^H. \quad (103)$$

Our analog beamformer design based on the weighted Frobenius norm minimization is very general. We can use Different weighting matrices to yield different analog beamformer matrices for realizing different performance tradeoffs. However, due to this weighting matrix in the objective function, in most case, it is challenging to compute the analog beamformer in a closed-form. To overcome this difficulty, the analog beamformer optimization problem is further transferred into the following optimization

$$\min_{\mathbf{F}_{AL,k}} \left\| \mathbf{D}_k^{-1} \mathbf{V}_{\mathcal{H}_k} \Sigma_{L,k} \mathbf{V}_{L,k}^H - \mathbf{F}_{AL,k} \right\|_F^2, \quad (104)$$

whose optimal solution can be directly computed by angle projection. This transformed problem is an ‘upper bound’ of the original problem (99), as shown in [27].

Given \mathbf{W}_k and \mathbf{D}_k , our algorithm to design the optimal analog transmit precoder for multi-hop AF relaying systems is summarized in Algorithm 1, where the objective function of (99) is $\Delta = \left\| \mathbf{W}_k^{\frac{1}{2}} (\mathbf{V}_{\mathcal{H}_k} \Sigma_{L,k} \mathbf{V}_{L,k}^H - \mathbf{D}_k \mathbf{F}_{AL,k}) \right\|_F^2$.

B. Analog Receive Combiner Design

Generally, based on Conclusions 4, 8 and 11, the auxiliary variables $\Pi_{R,k}$ for relays and Π_G for destination can be unified into a single form. Specifically, for a relay,

$$\Pi_{R,k} = (\bar{\mathbf{F}}_{AR,k} \bar{\mathbf{F}}_{AR,k}^H)^{-\frac{1}{2}} \bar{\mathbf{F}}_{AR,k}, \quad (105)$$

while for destination, we simply change $\Pi_{R,k}$ to Π_G and substitute $\bar{\mathbf{F}}_{AR,k}$ by \mathbf{G}_A in (105). Thus, we only need to discuss the design of analog receive combiner for a relay node. According to Section V, the main task here is to optimize

Algorithm 1 Analog Beamformer Optimization Algorithm

Input: Left singular matrix $\mathbf{V}_{\mathcal{H}_k}$, weight matrix \mathbf{W}_k , invertible matrix \mathbf{D}_k , iteration threshold ε

- 1: Set initial objective function of (99) to $\Delta = \varepsilon + 1 > \varepsilon$
- 2: Set initial $\mathbf{F}_{AL,k} = \mathcal{P}_{\mathcal{F}}(\mathbf{D}_k^{-1} \mathbf{V}_{\mathcal{H}_k})$, then calculate initial $\mathbf{V}_{L,k}$ from SVD (98)
- 3: **while** $\Delta > \varepsilon$ **do**
- 4: Update diagonal matrix $\Sigma_{L,k}$ using (100)
- 5: Compute unitary matrix $\mathbf{V}_{L,k}$ using (102)
- 6: Calculate analog beamformer matrix $\mathbf{F}_{AL,k}$ by solving (104) using phase projection
- 7: Compute Δ with new $\Sigma_{L,k}$, $\mathbf{V}_{L,k}$ and $\mathbf{F}_{AL,k}$
- 8: **end while**
- 9: **Return:** Optimal analog beamformer $\mathbf{F}_{AL,k}$

the analog receive combiner $\bar{\mathbf{F}}_{AR,k}$ so that the right singular matrix of the auxiliary variables $\Pi_{R,k}$ can match the right singular matrix of the preceding-hop channel.

By defining the SVD of the analog receive combiner

$$\bar{\mathbf{F}}_{AR,k} = \mathbf{U}_{R,k} \Sigma_{R,k} \mathbf{V}_{R,k}^H, \quad (106)$$

based on the previous work [27], the analog receive combiner design problem can be formulated as

$$\begin{aligned} \min_{\Sigma_{R,k}, \mathbf{U}_{R,k}, \bar{\mathbf{F}}_{AR,k}} \quad & \left\| \mathbf{W}_k^{\frac{1}{2}} (\mathbf{U}_{\mathcal{H}_k} \Sigma_{R,k} \mathbf{U}_{R,k}^H - \bar{\mathbf{F}}_{AR,k}^H) \right\|_F^2, \\ \text{s.t.} \quad & \mathbf{U}_{R,k} \in \mathcal{U}, \bar{\mathbf{F}}_{AR,k} \in \mathcal{F}_{PR,k}, \\ & \Sigma_{R,k} = \text{diag}\{\sigma_{R,1}, \dots, \sigma_{R,K}\}. \end{aligned} \quad (107)$$

It is worth noting that the optimization (107) has the identical form to the analog transmit precoder design problem (99). Therefore, the optimal closed-form diagonal matrix $\Sigma_{R,k}$ in (107) can be obtained as

$$\begin{aligned} \Sigma_{R,k} = & \left(\text{diag} \{ d[\mathbf{U}_{R,k}^H \mathbf{W}_k \mathbf{U}_{R,k}] \} \right)^{-1} \\ & \times \Re \left(\text{diag} \{ d[\mathbf{U}_{\mathcal{H}_k}^H \bar{\mathbf{F}}_{AR,k}^H \mathbf{W}_k \mathbf{U}_{R,k}] \} \right). \end{aligned} \quad (108)$$

Similarly, given the other variables, the left singular matrix $\mathbf{U}_{R,k}$ is obtained as [33]

$$\mathbf{U}_{R,k} = \mathbf{U}_U \mathbf{V}_U^H, \quad (109)$$

where the unitary matrices \mathbf{U}_U and \mathbf{V}_U are defined by the SVD

$$\bar{\mathbf{F}}_{AR,k} \mathbf{W}_k \mathbf{U}_{\mathcal{H}_k} \Sigma_{R,k} = \mathbf{U}_U \Sigma_U \mathbf{V}_U^H. \quad (110)$$

In particular, when the weight matrix \mathbf{W}_k is an identity matrix, the analog receive combiner design problem is simplified to

$$\begin{aligned} \min_{\bar{\mathbf{F}}_{AR,k}} \quad & \left\| \mathbf{U}_{\mathcal{H}_k} \Sigma_{R,k} \mathbf{U}_{R,k}^H - \bar{\mathbf{F}}_{AR,k}^H \right\|_F^2, \\ \text{s.t.} \quad & \bar{\mathbf{F}}_{AR,k} \in \mathcal{F}_{PR,k}. \end{aligned} \quad (111)$$

Therefore, the optimal solution of the analog receive combiner for (111) is obtained by phase projection as

$$\bar{\mathbf{F}}_{AR,k} = \mathcal{P}_{\mathcal{F}}(\mathbf{U}_{R,k} \Sigma_{R,k} \mathbf{U}_{\mathcal{H}_k}^H). \quad (112)$$

In general, the weight matrix \mathbf{W}_k is not an identity matrix, and in this case, the optimal solution of the analog receive combiner is much more complicated. But it is also interesting

to note that the solution (112) offers an ‘upper bound’ solution to this general optimal analog receive combiner.

Following the above discussions, it is clear that the analog receive combiner design for multi-hop AF relaying systems can also be completed using Algorithm 1, just as in the case of analog transmit precoder design.

VIII. NUMERAL RESULTS AND DISCUSSIONS

In order to assess the performance of the proposed solutions, several numerical results are presented. Without loss of generality, we investigate a three-hop AF MIMO relaying network. The source and destination are equipped with 32 antennas and 16 antennas, respectively. There are 4 RF chains involved in both the source and destination. The two relay nodes are both equipped with 32 antennas and 4 RF chains. From the source node, 4 data streams are transmitted. It is worth noting that our derivation does not rely on a particular channel model. To demonstrate this, in the simulation both millimeter wave (mmWave) channel and RF Rayleigh channel are considered. In the simulations, the noise power is equal at every node, and the system’s SNR is defined as the ratio of the transmit signal power at source and the noise power at destination, i.e., $\text{SNR} = P_{\text{Tx}}/\sigma_n^2$.

Three hybrid transceiver designs with unit-modulus constraints are compared, and they are our proposed robust hybrid transceiver optimization design (denoted by Proposed Alg.), the orthogonal matching pursuit based design (denoted as OMP Alg.) [13], [18], and the phase projection approximation based design (denoted as (Phase Alg.)). OMP Alg., originated from [13], is widely used in point-to-point or one-hop hybrid transceiver designs, and it is extended to two-hop relay systems in [18]. To the best of our knowledge, OMP Alg. applied to multi-hop scenarios has not been discussed in the existing literature. Based on the optimal structures presented in this paper and the optimal solution given in [4], we extend OMP Alg. to multi-hop scenarios. Specially, the codebook of OMP Alg. for a mmWave channel is given by the channel steering vectors, and the codebook of OMP Alg. for a RF channel is the same as that given in [27]. Phase Alg. is an efficient approximate hybrid transceiver design method, which is widely adopted [14], [27], [34]. Phase Alg. takes the phase projection of the ‘optimal’ analog beamformers without unit-modulus constraints as its analog transceiver solutions, i.e., $\mathbf{F}_{\text{AL},k} = \mathcal{P}_{\mathcal{F}}(\mathbf{D}_k^{-1}\mathbf{V}_{\mathbf{H}_k})$ and $\mathbf{F}_{\text{AR},k} = \mathcal{P}_{\mathcal{F}}(\mathbf{U}_{\mathbf{H}_k}^{\text{H}})$, and the least-square approximations of the optimal digital beamformers as its digital transceiver solutions, i.e., $\mathbf{F}_{\text{D},k} = (\mathbf{F}_{\text{AL},k}^{\text{H}}\mathbf{F}_{\text{AL},k})^{-1}\mathbf{F}_{\text{AL},k}^{\text{H}}\mathbf{F}_{\text{L},k}^{\text{opt}}\mathbf{F}_{\text{R},k}^{\text{opt}}\mathbf{F}_{\text{AR},k}^{\text{H}}(\mathbf{F}_{\text{AR},k}\mathbf{F}_{\text{AR},k}^{\text{H}})^{-1}$, in which $\mathbf{F}_{\text{L},k}^{\text{opt}}$ and $\mathbf{F}_{\text{R},k}^{\text{opt}}$ are the optimal left and right digital forward matrices. Furthermore, the powerful full digital transceiver design [4] (denoted as Full Digital) is used as the ultimate benchmark. Note that for the full digital design, the number of RF chains must match the number of antennas.

In Fig. 1, we compare the spectral efficiency performance of the four designs under the mmWave channel environment. Observe from Fig. 1 that the performance of our proposed robust hybrid transceiver design is very close to the optimal performance of the full digital design, and our design significantly outperforms the other two hybrid transceiver designs. It

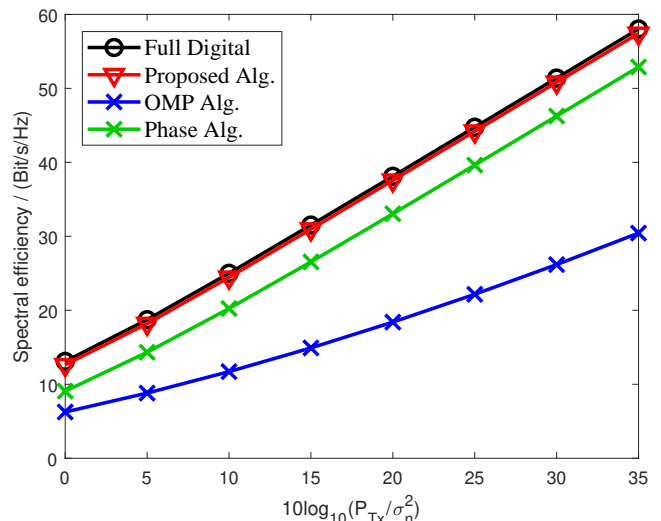


Fig. 1. Comparison of spectral efficiency for the three linear hybrid transceiver designs and the full digital design based on capacity maximization. The mmWave channel with $N_{\text{path}} = 10$ paths is used in the simulation.

is worth noting that OMP Alg., which performs very well in traditional point-to-point MIMO systems [13], [18], performs poorly for this three-hop AF relay MIMO system. This shows that the hybrid transceiver design based on OMP Alg. is not suitable for complicated multi-hop communication systems.

The results for the RF Rayleigh channel are depicted in Fig. 2. It can be seen that under the Rayleigh channel environment, our design only suffers from slight performance degradation, in comparison to the optimal full digital design, and the performance of our design is again significantly better than the other two hybrid designs. It is worth noting that OMP Alg. has a design challenge for Rayleigh channels, owing to the lack of steering vector based codebooks. Therefore, similar to [27], we have to use the phase matrix of Rayleigh channel as the OMP codebook.

Figs. 3 and 4 compare the MSE minimization performance of the four designs under the mmWave channel and

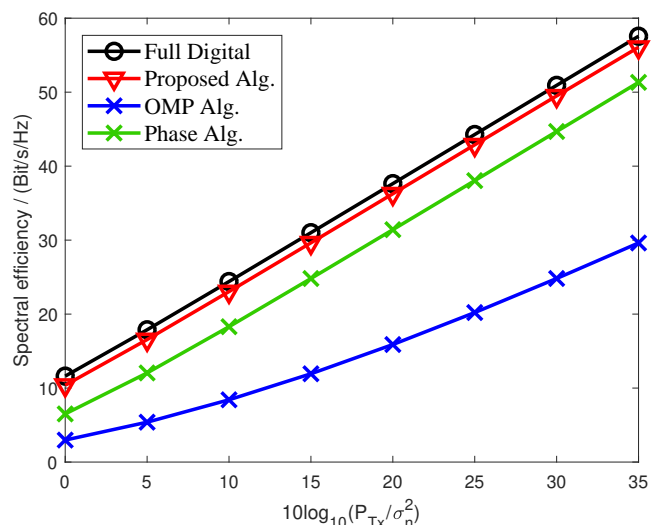


Fig. 2. Comparison of spectral efficiency for the three linear hybrid transceiver designs and the full digital design based on capacity maximization. The RF Rayleigh channel is used in the simulation.

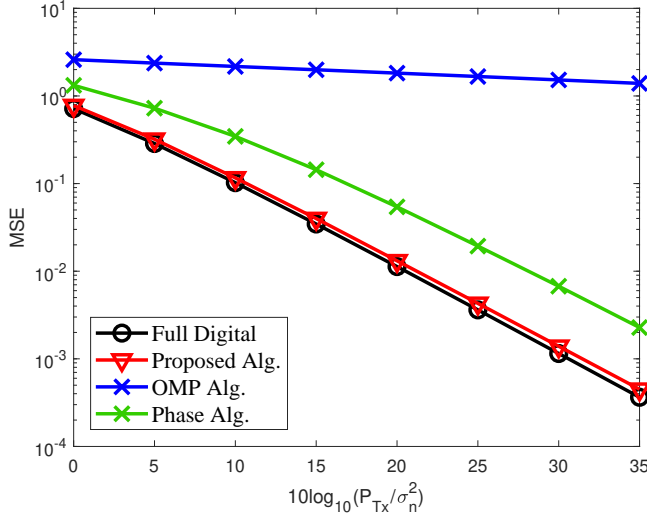


Fig. 3. Comparison of transmitted signal MSE for the three linear hybrid transceiver designs and the full digital design based on MSE minimization. The mmWave channel with $N_{\text{path}} = 10$ paths is used in the simulation.

RF Rayleigh channel environments, respectively. The results obtained again demonstrate that the achievable performance of our robust hybrid transceiver design is very close to the powerful full digital design, i.e., it is near optimal, while imposing substantially lower hardware costs. The results of Figs. 3 and 4 again show that hybrid transceiver design based on OMP Alg. is not suitable for multi-hop AF MIMO relaying networks.

Specially, the simulations mentioned above assume that there is no channel estimation error during hybrid transceiver designs. However, in reality, channel estimation errors may not be negligible. Thus, the channel estimation error is considered in the following simulation. In our simulation, transmit correlation matrix of channel error is given based on exponential model, which is $[\Psi_k]_{i,\ell} = \sigma_{e,k} \alpha_{e,k}^{|i-\ell|}$, where $[\Psi_k]_{i,\ell}$ is the element in i^{th} row and ℓ^{th} column of correlation matrix Ψ_k . Moreover, without loss of generality, it is assumed that

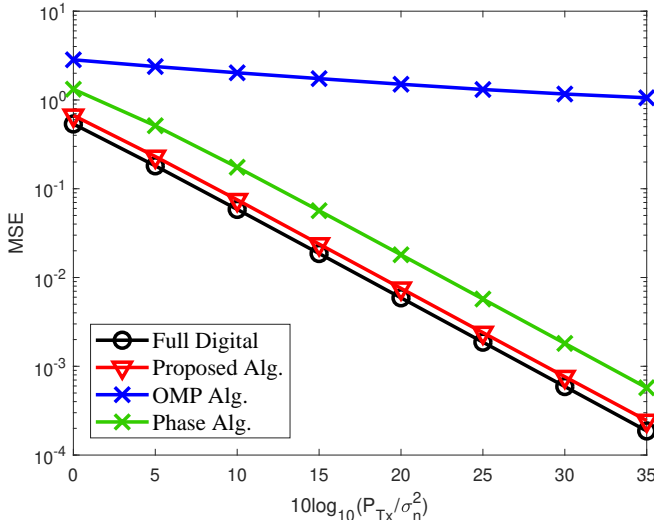


Fig. 4. Comparison of transmitted signal MSE for the three linear hybrid transceiver designs and the full digital design based on MSE minimization. The RF Rayleigh channel is used in the simulation.

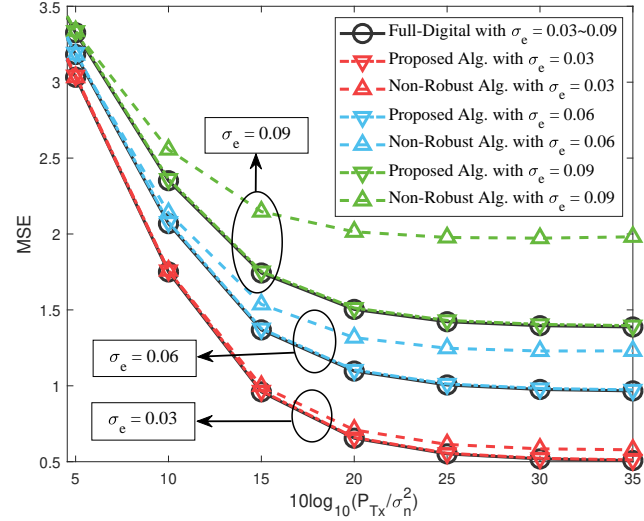


Fig. 5. Comparison of transmitted signal MSE under different channel estimation errors for the proposed robust hybrid transceiver design, the full digital robust transceiver design, and non-robust hybrid transceiver design based on MSE maximization with $\alpha_e = 0.6$. The RF Rayleigh channel is used in the simulation.

the correlation coefficients $\{\sigma_{e,k}\}$ and variances of transmit correlation matrix of channel error $\{\alpha_{e,k}\}$ are the same for each channel. For notational simplicity, the correlation coefficient and variance of transmit correlation matrix of channel error is denoted by σ_e and α_e , respectively, and $\alpha_e = 0.6$ is adopted in the following simulation.

Fig. 5 demonstrates the performance comparisons in terms of MSE between the proposed robust hybrid transceiver design, the full digital robust transceiver design [4], and non-robust hybrid transceiver design with different channel estimation errors. From Fig. 5, it can be seen that the proposed robust hybrid transceiver design has better performance than non-robust hybrid transceiver design with the existence of channel estimation errors. In addition, the performance of our proposed robust hybrid transceiver design is very close to that of the full digital robust transceiver design. Moreover, with the increase of channel estimation errors, the performance gap between our proposed robust hybrid transceiver design and non-robust hybrid transceiver design grows conspicuously. In other words, the proposed robust hybrid transceiver designs shows its superiority in various channel errors cases.

IX. CONCLUSIONS

In this paper, we have investigated robust hybrid transceiver optimization for multi-hop AF MIMO relaying networks, in which all nodes employ hybrid transceivers and multiple data streams are transmitted from source node simultaneously. Specifically, a unified design framework has been proposed for both hybrid linear and nonlinear transceivers under general objective functions, which also takes into account channel estimation error. Based on the proposed framework, the analog transceivers and digital transceivers can be decoupled with loss of optimality. Using matrix-monotonic optimization framework, the optimal structures of the analog and digital transceiver designs have been derived, which greatly simplify the hybrid transceiver optimizations. Based on the derived

optimal structures, both analog precoders and combiners as well as digital forward matrices can be optimized separately and efficiently. Simulation results obtained have demonstrated that our proposed robust hybrid transceiver design only suffers from a very slight performance loss compared to the powerful full digital design. This confirms that our hybrid transceiver design attains near optimal performance, while imposing substantially lower hardware cost than the full digital design.

REFERENCES

- [1] M. J. Farooq, H. ElSawy, and M.-S. Alouini, "A stochastic geometry model for multi-hop highway vehicular communication," *IEEE Trans. Wireless Commun.*, vol. 15, no. 3, pp. 2276–2291, 2016.
- [2] N. I. Miridakis, D. D. Vergados, and A. Michalas, "Dual-hop communication over a satellite relay and shadowed rician channels," *IEEE Trans. Veh. Technol.*, vol. 64, no. 9, pp. 4031–4040, 2015.
- [3] F. Ono, H. Ochiai, and R. Miura, "A wireless relay network based on unmanned aircraft system with rate optimization," *IEEE Trans. Wireless Commun.*, vol. 15, no. 11, pp. 7699–7708, 2016.
- [4] C. Xing, S. Ma, Z. Fei, Y.-C. Wu, and H. V. Poor, "A general robust linear transceiver design for multi-hop amplify-and-forward MIMO relaying systems," *IEEE Trans. Signal Process.*, vol. 61, no. 5, pp. 1196–1209, 2013.
- [5] C. Xing, F. Gao, and Y. Zhou, "A framework for transceiver designs for multi-hop communications with covariance shaping constraints," *IEEE Trans. Signal Process.*, vol. 63, no. 15, pp. 3930–3945, Feb. 2015.
- [6] C. Xing, Y. Ma, Y. Zhou, and F. Gao, "Transceiver optimization for multi-hop communications with per-antenna power constraints," *IEEE Trans. Signal Process.*, vol. 64, no. 6, pp. 1519–1534, Jan. 2016.
- [7] M. Peng, Q. Hu, X. Xie, Z. Zhao, and H. V. Poor, "Network coded multi-hop wireless communication networks: Channel estimation and training design," *IEEE J. Sel. Areas Commun.*, vol. 33, no. 2, pp. 281–294, 2015.
- [8] M. Mondelli, Q. Zhou, V. Lottici, and X. Ma, "Joint power allocation and path selection for multi-hop noncoherent decode and forward uwb communications," *IEEE Trans. Wireless Commun.*, vol. 13, no. 3, pp. 1397–1409, 2014.
- [9] D. Feng, C. Jiang, G. Lim, L. J. Cimini, G. Feng, and G. Y. Li, "A survey of energy-efficient wireless communications," *IEEE Commun. Surveys Tuts.*, vol. 15, no. 1, pp. 167–178, 2013.
- [10] S. Han, I. Chih-Lin, Z. Xu, and C. Rowell, "Large-scale antenna systems with hybrid analog and digital beamforming for millimeter wave 5G," *IEEE Commun. Mag.*, vol. 53, no. 1, pp. 186–194, 2015.
- [11] X. Zhang, A. F. Molisch, and S.-Y. Kung, "Variable-phase-shift-based RF-baseband codesign for MIMO antenna selection," *IEEE Trans. Signal Process.*, vol. 53, no. 11, pp. 4091–4103, 2005.
- [12] S. Kuttu and D. Sen, "Beamforming for millimeter wave communications: An inclusive survey," *IEEE Commun. Surveys Tuts.*, vol. 18, no. 2, pp. 949–973, 2016.
- [13] O. El Ayach, S. Rajagopal, S. Abu-Surra, Z. Pi, and R. W. Heath, "Spatially sparse precoding in millimeter wave MIMO systems," *IEEE Trans. Wireless Commun.*, vol. 13, no. 3, pp. 1499–1513, Mar. 2014.
- [14] W. Ni, X. Dong, and W.-S. Lu, "Near-optimal hybrid processing for massive MIMO systems via matrix decomposition," *IEEE Trans. Signal Process.*, vol. 65, no. 15, pp. 3922–3933, Aug. 2017.
- [15] T. E. Bogale, L. B. Le, A. Haghighat, and L. Vandendorpe, "On the number of RF chains and phase shifters, and scheduling design with hybrid analog-digital beamforming," *IEEE Trans. Wireless Commun.*, vol. 15, no. 5, pp. 3311–3326, 2016.
- [16] A. Alkhateeb, G. Leus, and R. W. Heath, "Limited feedback hybrid precoding for multi-user millimeter wave systems," *IEEE Trans. Wireless Commun.*, vol. 14, no. 11, pp. 6481–6494, 2015.
- [17] L. Zhao, D. W. K. Ng, and J. Yuan, "Multi-user precoding and channel estimation for hybrid millimeter wave systems," *IEEE J. Sel. Areas Commun.*, vol. 35, no. 7, pp. 1576–1590, 2017.
- [18] J. Lee and Y. H. Lee, "AF relaying for millimeter wave communication systems with hybrid RF/baseband MIMO processing," in *Proc. IEEE Int. Conf. Commun.*, Jun. 2014, pp. 5838–5842.
- [19] W. Xu, J. Liu, S. Jin, and X. Dong, "Spectral and energy efficiency of multi-pair massive MIMO relay network with hybrid processing," *IEEE Trans. Commun.*, vol. 65, no. 9, pp. 3794–3809, 2017.
- [20] X. Xue, Y. Wang, L. Dai, and C. Masouros, "Relay hybrid precoding design in millimeter-wave massive mimo systems," *IEEE Transactions on Signal Processing*, vol. 66, no. 8, pp. 2011–2026, 2018.
- [21] C. Lin, G. Y. Li, and L. Wang, "Subarray-based coordinated beamforming training for mmwave and sub-THz communications," *IEEE J. Sel. Areas Commun.*, vol. 35, no. 9, pp. 2115–2126, 2017.
- [22] D. Zhang, Y. Wang, X. Li, and W. Xiang, "Hybridly connected structure for hybrid beamforming in mmwave massive MIMO systems," *IEEE Trans. Commun.*, vol. 66, no. 2, pp. 662–674, 2018.
- [23] P. Raviteja, Y. Hong, and E. Viterbo, "Millimeter wave analog beamforming with low resolution phase shifters for multiuser uplink," *IEEE Trans. Veh. Technol.*, 2017.
- [24] Z. Li, S. Han, and A. F. Molisch, "Optimizing channel-statistics-based analog beamforming for millimeter-wave multi-user massive MIMO downlink," *IEEE Trans. Wireless Commun.*, vol. 16, no. 7, pp. 4288–4303, 2017.
- [25] J. Li, L. Xiao, X. Xu, and S. Zhou, "Robust and low complexity hybrid beamforming for uplink multiuser mmwave MIMO systems," *IEEE Commun. Lett.*, vol. 20, no. 6, pp. 1140–1143, 2016.
- [26] C. Xing, S. Ma, and Y. Zhou, "Matrix-monotonic optimization for MIMO systems," *IEEE Trans. Signal Process.*, vol. 63, no. 2, pp. 334–348, Jan. 2015.
- [27] C. Xing, X. Zhao, W. Xu, and X. Dong, "A framework for hybrid MIMO transceiver designs based on matrix-monotonic optimization," *arXiv Preprint*, 2018.
- [28] C. Xing, S. Li, Z. Fei, and J. Kuang, "How to understand linear minimum mean-square-error transceiver design for multiple-input-multiple-output systems from quadratic matrix programming," *IET Communications*, vol. 7, no. 12, pp. 1231–1242, 2013.
- [29] R. F. Fischer, *Precoding and signal shaping for digital transmission*. John Wiley & Sons, 2005.
- [30] C. Xing, M. Xia, F. Gao, and Y.-C. Wu, "Robust transceiver with Tomlinson-Harashima precoding for amplify-and-forward MIMO relaying systems," *IEEE J. Sel. Areas Commun.*, vol. 30, no. 8, pp. 1370–1382, Sep. 2012.
- [31] R. López-Valcarce, "Realizable linear and decision feedback equalizers: properties and connections," *IEEE Trans. Signal Process.*, vol. 52, no. 3, pp. 757–773, 2004.
- [32] C. Xing, Y. Jing, and Y. Zhou, "On weighted MSE model for MIMO transceiver optimization," *IEEE Trans. Veh. Technol.*, vol. 66, no. 8, pp. 7072–7085, 2017.
- [33] A. W. Marshall, I. Olkin, and B. C. Arnold, *Inequalities: theory of majorization and its applications*. Springer-Verlag New York, 2011.
- [34] R. Ratashekar and L. Hanzo, "Hybrid beamforming in mm-wave mimo systems having a finite input alphabet," *IEEE Transactions on Communications*, vol. 64, no. 8, pp. 3337–3349, 2016.